

# Partition functions 1: Improved partition functions and thermodynamic quantities for normal, equilibrium, and ortho and para molecular hydrogen<sup>★</sup>

A. Popovas<sup>1,★★</sup> and U. G. Jørgensen<sup>1</sup>

1. Niels Bohr Institute & Centre for Star and Planet Formation, University of Copenhagen, Øster Voldgade 5-7, 1350 Copenhagen K, Denmark e-mail: popovas@nbi.ku.dk

Received August 19, 2015; accepted July 1, 2016

## ABSTRACT

*Context.* Hydrogen is the most abundant molecule in the Universe. Its thermodynamic quantities dominate the physical conditions in molecular clouds, protoplanetary disks, etc. It is also of high interest in plasma physics. Therefore thermodynamic data for molecular hydrogen have to be as accurate as possible in a wide temperature range.

*Aims.* We here rigorously show the shortcomings of various simplifications that are used to calculate the total internal partition function. These shortcomings can lead to errors of up to 40 percent or more in the estimated partition function. These errors carry on to calculations of thermodynamic quantities. Therefore a more complicated approach has to be taken.

*Methods.* Seven possible simplifications of various complexity are described, together with advantages and disadvantages of direct summation of experimental values. These were compared to what we consider the most accurate and most complete treatment (case 8). Dunham coefficients were determined from experimental and theoretical energy levels of a number of electronically excited states of H<sub>2</sub>. Both equilibrium and normal hydrogen was taken into consideration.

*Results.* Various shortcomings in existing calculations are demonstrated, and the reasons for them are explained. New partition functions for equilibrium, normal, and ortho and para hydrogen are calculated and thermodynamic quantities are reported for the temperature range 1 - 20000 K. Our results are compared to previous estimates in the literature. The calculations are not limited to the ground electronic state, but include all bound and quasi-bound levels of excited electronic states. Dunham coefficients of these states of H<sub>2</sub> are also reported.

*Conclusions.* For most of the relevant astrophysical cases it is strongly advised to avoid using simplifications, such as a harmonic oscillator and rigid rotor or ad hoc summation limits of the eigenstates to estimate accurate partition functions and to be particularly careful when using polynomial fits to the computed values. Reported internal partition functions and thermodynamic quantities in the present work are shown to be more accurate than previously available data.

**Key words.** Thermodynamic quantities – Hydrogen – Partition function – Dunham coefficients

## 1. Introduction

The total internal partition function,  $Q_{tot}(T)$ , is used to determine how atoms and molecules in thermodynamic equilibrium are distributed among the various energy states at particular temperatures. It is the statistical sum over all the Boltzmann factors for all the bound levels. If the particle is not isolated, there is an occupation probability between 0 and 1 for each level depending on interactions with its neighbours. Together with other thermodynamic quantities, partition functions are used in many astrophysical problems, including equation of state, radiative transfer, dissociation equilibrium, evaluating line intensities from spectra, and correction of line intensities to temperatures other than given in standard atlases. Owing to the importance of  $Q_{tot}(T)$ , a number of studies were conducted throughout the past several decades to obtain more accurate values and present them in a convenient way. It is essential that a standard coherent set of  $Q_{tot}(T)$  is being used for any meaningful astrophysical con-

clusions from calculations of different atmospheric models and their comparisons.

Unfortunately, today we face a completely different situation. We have noted that most studies give more or less different results, sometimes the differences are small, but sometimes they are quite dramatic, for instance when different studies used different conventions to treat nuclear spin states (and later do not strictly specify these) or different approximations, cut-offs, etc. Furthermore, different methods of calculating the  $Q_{tot}(T)$  are implemented in different codes, and it is not always clear which methods in particular are used. Naturally, differences in  $Q_{tot}(T)$  values and hence in their derivatives (internal energy, specific heat, entropy, free energy) result in differences in the physical structure of computed model atmosphere even when line lists and input physical quantities (e.g.  $T_{eff}$ ,  $\log g$ , and metallicities) are identical.

In the subsequent sections we review how  $Q_{tot}(T)$  is calculated, comment on which simplifications, approximations, and constraints are used in a number of studies, and show how they compare to each other. We also argue against using molecular constants to calculate the partition functions. The molecular constants are rooted in the semi-classical idea that the vibrational

<sup>★</sup> Tables 25 to 28 are only available in electronic form at the CDS via anonymous ftp to cdsarc.u-strasbg.fr (130.79.128.5) or via <http://cdsweb.u-strasbg.fr/cgi-bin/qcat?J/A+A/>

<sup>★★</sup> Corresponding author.

rotational eigenvalues can be expressed in terms of a modified classical oscillator-rotor analogue. This erroneous concept has severe challenges at the highest energy levels that are not avoided by instead making a simple summation of experimentally determined energy levels, simply due to the necessity of naming the experimental levels by use of assigned quantum numbers. Instead, we report Dunham(11) coefficients for the ground electronic state and a number of excited electronic states, as well as resulting partition functions and thermodynamic quantities. The Dunham coefficients are not rooted in the classical picture, but still use quantum number assignments of the energy levels, and this approach is also bound to the same challenges of defining the upper energy levels in the summation, as is the summation using molecular constants (and/or pure experimental data). No published studies have solved this challenge yet, but we quantify the uncertainty it implies on the resulting values of the chemical equilibrium partition function.

## 2. Energy levels and degeneracies

In the Born-Oppenheimer approximation (6) it is assumed that the rotational energies are independent of the vibrational energies, and the latter are independent of the electronic energies. Then the partition function can be written as the product of separate contributors - the external (i.e. translational) partition function, and the rotational, vibrational, and electronic partition functions.

### 2.1. Translational partition function

The  $Q_{tr}$  can be expressed analytically as

$$Q_{tr} = \frac{Nk_B T}{\lambda^3 P}, \quad (1)$$

where

$$\lambda = \sqrt{\frac{2\pi\hbar^2}{mk_B T}}, \quad (2)$$

and  $N$  is the number of particles,  $k_B$  is Boltzmann's constant,  $P$  is the pressure, and  $m$  the mass of the particle. The rest of this section considers the internal part,  $Q_{int}$ .

### 2.2. Vibrational energies

The energy levels of the harmonic oscillator (HO)

$$E(v) = \left(v + \frac{1}{2}\right)h\omega \quad (3)$$

depend on the integer vibrational quantum number  $v = 0, 1, 2, \dots$ . These energy levels are equally spaced by

$$\Delta E = h\omega. \quad (4)$$

The frequency  $\omega = \frac{1}{2\pi} \sqrt{k/\mu}$  depends on the constant  $k$ , which is the force constant of the oscillator, and  $\mu$ , the reduced mass of the molecule. The lowest vibrational level is  $E = \frac{1}{2}h\omega$ . The harmonic oscillator potential approximates a real diatomic molecule potential well enough in the vicinity of the potential minimum at  $R = R_e$ , where  $R$  is the internuclear distance and  $R_e$  is the equilibrium bond distance, but it deviates increasingly for larger  $|R - R_e|$ . A better approximation is a Morse potential,

$$E_{pot}(R) = E_D \left[1 - e^{-a(R-R_e)}\right]^2, \quad (5)$$

where  $E_D$  is the dissociation energy of the rigid molecule. The experimentally determined dissociation energy  $E_D^{exp}$ , where the molecule is dissociated from its lowest vibration level, has to be distinguished from the binding energy  $E_B$  of the potential well, which is measured from the minimum of the potential. The difference is  $E_D^{exp} = E_B - \frac{1}{2}h\omega$ . The energy eigenvalues are

$$E(v) = h\omega \left(v + \frac{1}{2}\right) - \frac{h^2\omega^2}{4E_D} \left(v + \frac{1}{2}\right)^2 \quad (6)$$

with energy separations

$$\Delta E(v) = E(v+1) - E(v) = h\omega \left[1 - \frac{h\omega}{2E_D}(v+1)\right]. \quad (7)$$

When using a Morse potential, the vibrational levels are clearly no longer equidistant: the separations between the adjacent levels decrease with increasing vibrational quantum number  $v$ , in agreement with experimental observations. In astrophysical applications these energies are commonly expressed in term-values  $G(v) = E(v)/hc$ , and the vibrational energies in the harmonic case are then given as

$$G(v) = \omega_e \left(v + \frac{1}{2}\right), \quad (8)$$

and in the anharmonic case are given (when second-order truncation is assumed) as

$$G(v) = \omega_e \left(v + \frac{1}{2}\right) - \omega_e x_e \left(v + \frac{1}{2}\right)^2, \quad (9)$$

where  $\omega_e = \frac{\omega}{c}$  is the harmonic wave number,  $\omega_e x_e = \frac{h\omega^2}{4cE_D} = \omega_e^2 \frac{hc}{4E_D}$  is the anharmonicity term, and  $\omega = a\sqrt{2E_D/\mu}$  is the vibrational frequency. We remark that literally, only  $\omega$  is a frequency (measured in  $s^{-1}$ ), while  $\omega_e$  is a wave number (measured in  $cm^{-1}$ ), but in the literature  $\omega_e$  is commonly erroneously called a frequency any way. In the harmonic approximation, the Boltzmann factor (i.e. the relative population of the energy levels) can be summed analytically from  $v = 0$  to  $v = \infty$  (22),

$$Q_v \approx \sum_{v=0}^{\infty} e^{-hc\omega_e(v+\frac{1}{2})/k_B T} = (1 - e^{-hc\omega_e/k_B T})^{-1}. \quad (10)$$

### 2.3. Rotational energies

In the rigid rotor approximation (RRA), a diatomic molecule can rotate around any axis through the centre of mass with an angular velocity  $\omega_\perp$ . Its rotation energy is

$$E(J) = \frac{1}{2}I\omega_\perp^2 = \frac{J^2}{2I}, \quad (11)$$

here  $I = \mu R^2$  is the moment of inertia of the molecule with respect to the rotational axis and  $|J| = I\omega_\perp$  is its rotational angular momentum. In the simplest quantum mechanical approximation, the square of the classical angular momentum is substituted by  $J(J+1)$ ,

$$|J|^2 \rightarrow J(J+1)\hbar^2$$

and the rotational quantum number  $J$  can take only discrete values. The rotational energies of a molecule in its equilibrium position are therefore represented by a series of discrete values

$$E(J) = \frac{J(J+1)\hbar^2}{2I}, \quad (12)$$

and the energy separation between adjacent rotational levels

$$\Delta E(J) = E(J+1) - E(J) = \frac{(J+1)\hbar^2}{2I} \quad (13)$$

is increasing linearly with  $J$ . Rotational term-values are

$$F(J) = \frac{J(J+1)\hbar^2}{8\pi^2 I} = B_e J(J+1), \quad (14)$$

where

$$B_e = \frac{\hbar^2}{8\pi^2 c I} \quad (15)$$

is the main rotational molecular constant and  $F(J)$  is measured in the same units as  $G(v)$ , that is,  $\text{cm}^{-1}$ . A mathematical advantage (but physically erroneous) of Eq. 14 is that the rotational partition function  $Q_{rot}$  can be calculated analytically,

$$Q_{rot} \approx \int (2J+1) e^{-hcB_e J(J+1)/kT} dJ = \frac{kT}{hcB_e}. \quad (16)$$

A slightly more general approximation would be a non-rigid rotor. In this case, when the molecule rotates, the centrifugal force,  $F_c = \mu\omega^2 R \approx \mu\omega_c^2 R_e$ , acts on the atoms and the internuclear distance widens to a value  $R$  that is longer than  $R_e$ , and then the rotation energies are expressed as

$$E(J) \approx \frac{J(J+1)\hbar^2}{2I} - \frac{J^2(J+1)^2\hbar^4}{2k\mu^2 R_e^6}, \quad (17)$$

where  $k = 4\pi^2\omega_c^2 c^2 \mu$  is the restoring force constant in a harmonic oscillator approximation, introduced above.

For a given value of the rotational quantum number  $J$  the centrifugal widening makes the moment of inertia larger and therefore the rotational energy lower, as expressed in Eq. (17). This effect compensates for the increase in potential energy. Using term-values, a centrifugal distortion constant  $D_e$  is introduced into Eq. (14), yielding

$$F(J) = B_e J(J+1) - D_e J^2(J+1)^2. \quad (18)$$

It is often assumed that two terms are enough to have a good approximation and that more terms only give a negligible effect on the partition function. Unfortunately, this is rarely the case. When higher vibrational and rotational states are taken into consideration, as we show in the subsequent sections, higher order terms must be used. The rotational partition function  $Q_{rot}$  can be computed in the same way as the vibrational partition function. However, there are  $2J+1$  independent ways the rotational axis can orient itself in space with the same given energy. Furthermore, a symmetry factor,  $\sigma$ , has to be added as well if no full treatment of the nuclear spin degeneracy is included. In this case, oppositely oriented homonuclear molecules are indistinguishable, and half of their  $2J+1$  states are absent. Hence  $\sigma$  is 2 for homonuclear molecules and unity for heteronuclear molecules, and this leads to half as many states in homonuclear molecules as in corresponding heteronuclear molecules, such that Eq. (16) becomes

$$Q_{rot} = \frac{kT}{\sigma hc B_e}. \quad (19)$$

In the full spin-split degeneracy treatment for homonuclear molecules, the degeneracy factor is given by

$$g_n = (2S_1 + 1)(2S_2 + 1) \quad (20)$$

for the possible orientations of the nuclear spins  $S_1$  and  $S_2$ . For the two nuclei, each with spin  $S$ , there are  $S(2S+1)$  antisymmetric spin states and  $(S+1)(2S+1)$  symmetric ones. For diatomic molecules, composed of identical Fermi nuclei<sup>1</sup>, the spin-split degeneracy for even and odd  $J$  states are

$$g_{n,even} = [(2S+1)^2 + (2S+1)]/2, \quad (21)$$

$$g_{n,odd} = [(2S+1)^2 - (2S+1)]/2$$

respectively. The normalisation factor for  $g_n$  is  $1/(2S+1)^2$ . For identical Bose nuclei<sup>2</sup>, the spin-split degeneracy for even and odd  $J$  states are opposite to what they are for Fermi systems.

#### 2.4. Interaction between vibration and rotation

Interaction between vibrational and rotational motion can be allowed by using a different value of  $B_v$  for each vibrational level:

$$B_v = B_e - \alpha_e(v + \frac{1}{2}), \quad (22)$$

where  $\alpha_e$  is the rotation-vibration interaction constant.

#### 2.5. Electronic energies

The excited electronic energy levels typically are at much higher energies than the pure vibrational and rotational energy levels. For molecules they therefore contribute only a fraction to the partition function. Bohn & Wolf (4, 1984) points out that for molecules the electronic state typically is non-degenerate because the electronic energy is typically higher than the dissociation energy, so that  $Q_{el} = 1$ . Although this is the case for most molecules, others do have degenerate states, therefore  $Q_{el}$  is sometimes fully calculated nonetheless. Naturally, molecules can and do occupy excited electronic states, as many experiments show. The electronic partition function is expressed as

$$Q_{el} = \sum \tilde{\omega}_e e^{-T_e/k_B T}, \quad (23)$$

where  $\tilde{\omega}_e = (2 - \delta_{0,\Lambda})(2S+1)$  is the electronic statistical weight, where  $\delta_{i,j}$  is the Kronecker delta symbol, which is 1 if  $\Lambda = 0$  and 0 otherwise.

#### 2.6. Vibrational and rotational energy cut-offs and the basic concept of quantum numbers

If the semi-classical approach to the very high eigenstates (where this approximation has already lost its validity) is maintained by assigning  $v$  and  $J$  quantum numbers either as reached from the Morse potential (Eq. (7)) or from introducing second-order terms (as is most common), then the absurdity in the approach becomes more and more obvious. In Herzberg's pragmatic interpretation (21, , p. 99-102) the classical theory is applied until the dissociation energy is reached (which for  $H_2$  corresponds to  $v = 14$ ), and then  $v$  values are disregarded above this. Other authors have not always been happy with this interpretation, however, and insisted on including  $v$  values well above the dissociation energy to a somewhat arbitrary maximum level, which affects the value of the partition function substantially at high temperatures. In the Morse potential (Eq. (7)) the vibrational eigenstates can in principle be counted up to  $v$  quantum numbers corresponding to

<sup>1</sup>  $S=1/2, 3/2, 5/2, \dots$

<sup>2</sup>  $S=0, 1, 2, \dots$

approximately twice the dissociation energy, and for even higher  $v$  quantum numbers, the vibrational energy becomes a decreasing function of the increasing  $v$  number:

$$\Delta E(v) = h\omega \left[ 1 - \frac{h\omega}{2E_D}(v+1) \right] < 0, \quad (24)$$

solving for  $v$  where  $\Delta E(v)$  first becomes lower than or equal to 0, we obtain

$$v_{\max} = \frac{2E_D - h\omega}{h\omega}. \quad (25)$$

The next level,  $v_{\max} + 1$ , would produce zero or even negative energy addition. To solve this failure, more terms are needed to better approximate the real potential. Expressing  $v_{\max}$  in vibrational term molecular constants, we obtain

$$v_{\max} = \frac{2E_D - h\omega}{h\omega} = \frac{\omega}{c} \frac{8cE_D}{2h\omega^2} = \frac{\omega_e}{2\omega_e x_e} - 1. \quad (26)$$

$v_{\max}$  is sometimes used as a cut-off level for summation of vibrational energies (e.g. (25)).

The classical non-rigid rotor approximation, Eq. (18) also shows that the energy between adjacent levels decreases with increasing  $J$ , thus writing Eq. (18) for  $J$  and  $J+1$  states and making the difference between eigenstates equal to zero,

$$B_e(J+1)(J+2) - D_e(J+1)^2(J+2)^2 - B_e J(J+1) + D_e J^2(J+1)^2 = 0, \quad (27)$$

and solving for  $J$ , we obtain the maximum rotational number,

$$J_{\max} = \frac{\sqrt{2} \sqrt{B_e} - 2 \sqrt{D_e}}{2 \sqrt{D_e}}. \quad (28)$$

The summation over rotational energies is commonly cut-off at some arbitrary rotational level or is approximated by an integral from 0 to  $\infty$ . When examining the literature, we did not note this  $J_{\max}$  expression. As with the non-harmonic oscillator, adding more terms to the non-rigid rotor approximation would give a better approximation. Now it is possible to measure more terms ( $\omega_y e_y, \omega_z e_z, \dots$  for vibrational levels,  $H_e$  for rotational levels). Although they are important for high-temperature molecular line lists and partition functions, they are often calculated only from energy levels measured in the vicinity of the bottom of the potential well. For higher  $v$  and  $J$  values, the resulting energies can therefore still deviate from experimentally determined energy term values. Furthermore, the whole concept of quantum numbers  $v$  and  $J$  and associated degeneracies etc. of course relates to the classical approximations in quantum theory, which breaks down at energies far from the validity of a description of the molecule as a rotating system of some kind of isolated atoms bound to one another by some kind of virtual spring. This shows that there is an unclear limit beyond which it is no longer meaningful to continue adding higher order terms to expand the simple quantum number concept to fit the highest measured energy levels. At these highest levels there is nothing other than the mathematical wavefunction itself that represent reality in a meaningful way.

Given these limitations in defining the uppermost levels in a meaningful way within the semi-classical quantum mechanics, the question is whether in the end it is not more accurate to use only experimental energy levels in the construction of the partition function. However, exactly for the uppermost levels there is no such concept as experimentally determined energy levels

summed to a partition function. The first problem is the practical one that for no molecule all the levels have been measured. For any missing level an assumption has to be applied, which could be to exclude the level in the summation, to make a linear fit of its energy between the surrounding measured energy levels, or to construct some type of polynomial fit from which to determine the missing levels, which would then be based on a choice of harmonic or anharmonic and rigid or non-rigid rotor or other polynomial fits. Another practical limitation is that experimentally, energy levels beyond the molecular dissociation energy would be seen. These levels can either give rise to a photo-dissociation of the molecule or relax back into a bound state, each with a certain probability. To construct a meaningful partition function, it would therefore at best have to be both temperature and pressure dependent, taking into account the timescales for molecular dissociation and recombination. An even more fundamental problem in defining a partition function based on experimental data is that each observed energy level has to be ‘‘named’’. This naming is done by assigning a quantum number, which associates the measurements to a chosen semi-classical theory, however, and the quantum numbers associated with the state determines the degeneracy that the summation in the partition function will be multiplied with. This dilemma becomes perhaps more clear for slightly larger molecules than  $H_2$  where the degeneracy of the bending mode is multiplied directly into the partition function, but is a non-trivial function of the assigned vibrational quantum number of the state ((40)), while at the same time quantum mechanical ab initio calculations show that the wavefunction of the uppermost states can only be expressed as a superposition of several wavefunctions that are expressed by each their set of quantum numbers ((27)), such that there is no ‘‘correct’’ assignment of the degeneracy factor that goes into the ‘‘experimental’’ partition function. There have been various ways in the literature to circumvent this problem. The most common is to ignore it. In some cases (e.g. (25) and (28)) it was chosen to first complement the ‘‘experimental’’ values with interpolation between the measured values and then add extrapolated values above the dissociation energy (ignoring the pressure dependence) based on polynomial fits to the lower levels, with a cut-off of the added levels determined by where the order of the fit caused energy increments of further states to become negative (determined e.g. from Eqs. (25) and (28)). For low temperatures these inconsistencies have no practical implication because the somewhat arbitrarily added eigenstates do not contribute to the final partition function within the noise level. For higher temperatures, however, the uncertainty due to the inconsistency of how to add energy levels above the dissociation energy becomes larger than the uncertainty in using a polynomial fit, rather than the actually computed values, as illustrated in Fig. 1. Realising that strictly speaking there is no such concept as an experimentally summed partition function, and there is no ‘‘correct’’ upper level, we decided for a hybrid model, where the uppermost energy level in our summations are the minimum of the last level before the dissociation energy and the level where the energy increments become negative according to Eqs. (38) and (39), see case 8 in the next section for more details. For high temperatures this approach will give results in between the results that would be obtained by a cut at the dissociation energy of the ground electronic state and an upper level determined by Eqs. (38) and (39), or a more experimentally inspired upper level (black curve), as is illustrated in Fig. 1. The difference between the three methods (upper cuts) is an illustration of the unavoidable uncertainty in the way the partition functions can be calculated today. In the future, computers may be powerful enough to make sufficiently

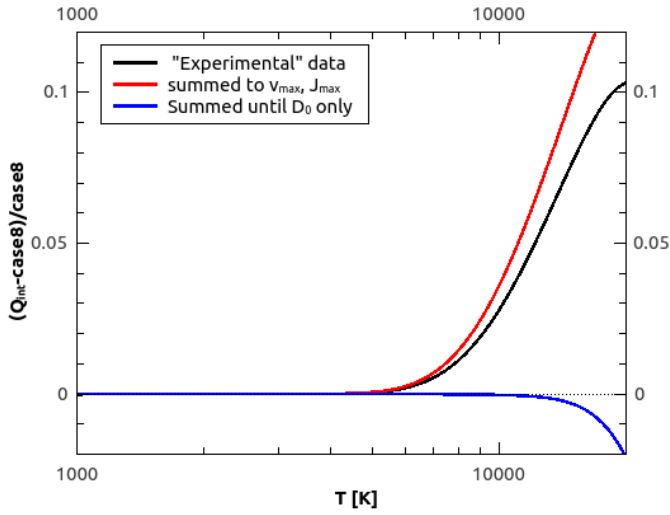


**Fig. 1.** Difference between different methods used to stop the summation (upper cuts) of the partition function. Different cut-offs are compared to the partition function obtained from case 8 (see text for more details), which is the zero line. The curve marked “experimental “ data is derived by summing the Boltzmann factor of experimental data for the ground state used in (28)<sup>3</sup>. The blue curve is the summation for the ground electronic state summed to  $D_0$  only. The red curve is the corresponding summation of energy levels of the three lowest electronic states based on Dunham coefficients and with a cut-off according to Eqs. (38) and (39).

accurate ab initio calculations of these uppermost energy levels (but today the upper part of the ab initio energy surface is most often fitted to the experiments rather than representing numerical results).

There are no restrictions on the number of energy eigenstates available for an isolated molecule before dissociation. However, the physical conditions of a thermodynamic system impose restrictions on the number of possible energy levels through the mean internal energy (7; 44). A molecule in a thermodynamic system is subjected to the interaction with other molecules through collisions and with the background energy that permeates the system, making the number of energy states available dependent on the physical conditions of the system. From a geometric point of view, in a thermodynamic system with total number density of particles  $N$ , the volume occupied by each molecule considering that the volume is cubic and of side  $L$ , is  $L^3 = 1/N$ . This imposes a maximum size that the molecule may have without invading the space of other molecules, and therefore the number of states becomes finite. From a physical point of view, the number of energy states of the molecules is delimited by the interactions with the rest of the system since the energy state above the last one becomes dissociated by the mean background thermal energy of the system under study. Hence the maximum number of states available for a particle is dependent on the properties of the surrounding system. (8) have shown that in a dense medium ( $N \geq 10^{21} \text{ cm}^{-3}$ ) interaction between molecules and their surroundings starts to become important and that the physical approach dominates the geometrical one. They also derived equations for the maximum vibrational and rotational levels in such conditions, assuming the rigid rotor approximation.

<sup>3</sup> listed at <http://kurucz.harvard.edu/molecules/h2/eleroyh2.dat>

### 3. Simplifications used in other studies

In this section we briefly review the simplifications in calculating  $Q_{int}$  that have been used and how they compare to each other.

#### 3.1. Case 1.

This is the simplest case that is often given in textbooks: a simple product of harmonic oscillator approximation (HOA) and rigid rotor approximation (RRA), respectively summed and integrated to infinity, assuming Born-Oppenheimer approximation without interaction between vibration and rotation, and assuming that only the ground electronic state is present.  $Q_{int}$  then becomes a simple product of Eqs. (10) and (26):

$$Q_{int} = \frac{T}{c_2 \sigma B_e} \frac{1}{1 - \exp(-c_2 \omega_e / T)}, \quad (29)$$

where  $c_2 = hc/k_B$  is the second radiation constant.

#### 3.2. Case 2.

This time, HOA is dropped.  $v_{max}$  is evaluated by Eq. (25)<sup>4</sup>, only ground electronic state and no upper energy limit are assumed:

$$Q_{int} = \exp \left[ \frac{c_2}{T} \left( \frac{\omega_{e,1}}{2} - \frac{\omega_e x_{e,1}}{4} \right) \right] \frac{T}{\sigma c_2 B_e} \sum_{v=0}^{v_{max}} \exp \left[ \frac{c_2}{T} \omega_e \left( v + \frac{1}{2} \right) - \omega_e x_e \left( v + \frac{1}{2} \right)^2 \right], \quad (30)$$

where the first term refers to the lowest vibrational level of the ground state instead of the bottom of the potential well.

#### 3.3. Case 3.

This is the same as case 2, but this time  $B_e$  in Eq. 30 is replaced by  $B_v$ , obtained by Eq. (22) (i.e. the Born-Oppenheimer approximation is abandoned):

$$Q_{int} = \exp \left[ \frac{c_2}{T} \left( \frac{\omega_{e,1}}{2} - \frac{\omega_e x_{e,1}}{4} \right) \right] \sum_{v=0}^{v_{max}} \frac{T}{\sigma c_2 B_v} \exp \left[ \frac{c_2}{T} \omega_e \left( v + \frac{1}{2} \right) - \omega_e x_e \left( v + \frac{1}{2} \right)^2 \right]. \quad (31)$$

#### 3.4. Case 4.

This is the same as case 3, but this time an arbitrary energy truncation for the vibrational energy is added. The most commonly used (42; 38; 37; 13; 20; 14; 12) value is  $40000 \text{ cm}^{-1}$ :

$$Q_{int} = \exp \left[ \frac{c_2}{T} \left( \frac{\omega_{e,1}}{2} - \frac{\omega_e x_{e,1}}{4} \right) \right] \sum_{v=0}^{v_{max}=40000 \text{ cm}^{-1}} \frac{T}{\sigma c_2 B_v} \exp \left[ \frac{c_2}{T} \omega_e \left( v + \frac{1}{2} \right) - \omega_e x_e \left( v + \frac{1}{2} \right)^2 \right]. \quad (32)$$

#### 3.5. Case 5.

In this case, excited electronic states are added,

$$Q_{int} = \exp \left[ \frac{c_2}{T} \left( \frac{\omega_{e,1}}{2} - \frac{\omega_e x_{e,1}}{4} \right) \right] \sum_e^{T_e, max} \sum_{v=0}^{v_{max}} \frac{\tilde{\omega}_e T}{\sigma c_2 B_v} \exp \left[ \frac{c_2}{T} \omega_e \left( v + \frac{1}{2} \right) - \omega_e x_e \left( v + \frac{1}{2} \right)^2 + T_e \right], \quad (33)$$

<sup>4</sup> Which has no physical meaning

where  $T_{e,max} = 40000 \text{ cm}^{-1}$ .

### 3.6. Case 6.

This case provides the full treatment: we finally drop the RRA. As in cases 3 - 5, this case also fully abandons the Born-Oppenheimer approximation because electronic and vibrational and rotational states are interacting and depend on one another. Different vibrational and rotational molecular constants are used for the different electronic levels. Furthermore, the arbitrary truncation is dropped and the real molecular dissociation energy,  $D_0$ , is used for the ground state. In principle, molecules can occupy eigenstates above the dissociation energy, but they are not stable and dissociate almost instantly or relax to lower states below the dissociation level. Since the timescale for dissociation is usually shorter than for relaxation, molecules tend to dissociate rather than relax. Furthermore, a pre-dissociation state is usually present for molecules, where no eigenstates can be distinguished and a continuum of energies is present. This regime is beyond the scope of this work. For excited electronic states the ionisation energy is used instead of the dissociation energy. The equation for the full treatment takes the form

$$Q_{int} = \exp\left[\frac{c_2}{T}\left(\frac{\omega_{e,1}}{2} - \frac{\omega_e x_{e,1}}{4}\right)\right] \sum_{e=0}^{T_{e,max}} \sum_{v=0}^{v_{max}} \sum_{J=0}^{J_{max}} \tilde{\omega}_e(2J+1) \exp\left[\frac{-c_2}{T}(T_e + G_v + F_J)\right], \quad (34)$$

where  $G_v$  is calculated as in Eq. (9),  $F_J = B_v J(J+1) - D_v J^2(J+1)^2$ , where  $B_v$  is calculated as in Eq. (22), and  $D_v = D_e - \beta_e(v + \frac{1}{2})$ .  $T_{e,max}$  is the term energy of the highest excited electronic state and is taken into account. For each electronic state the  $v$  and  $J$  quantum numbers are summed to a maximum value that corresponds to the dissociation energy of that particular electronic state.

### 3.7. Case 7.

For homonuclear molecules, nuclear spin-split degeneracy must also be taken into account. In this case, the form of the equation is

$$Q_{int} = \exp\left[\frac{c_2}{T}\left(\frac{\omega_{e,1}}{2} - \frac{\omega_e x_{e,1}}{4}\right)\right] \sum_{e=0}^{e_{max}} \sum_{v=0}^{v_{max}} \sum_{J=0}^{J_{max}} \tilde{\omega}_e g_n(2J+1) \exp\left[\frac{-c_2}{T}(T_e + G_v + F_J)\right], \quad (35)$$

where  $g_n$  is calculated as in Eq. (21).

### 3.8. Case 8.

This is the most accurate model we present here. Although cases 6 and 7 give reasonable results, they are still not sufficient at high temperatures. Molecular constants are conceptually rooted in classical mechanics (such as force constants of a spring and centrifugal distortion), and most often they are evaluated only from lower parts of the potential well and represent higher states poorly. For this reason it is more accurate to use a Dunham polynomial (11) to evaluate energy levels,

$$T_{Dun} = \sum_{i,k=0}^{i_{max},k_{max}} Y_{ik} \left(v + \frac{1}{2}\right)^i (J(J+1))^k, \quad (36)$$

where  $Y_{ik}$  are Dunham polynomial fitting constants. These constants are not exactly related to classical mechanical concepts, such as bond lengths and force constants, and as such represent one step further into modern quantum mechanics. The lower order constants have values very close to the corresponding classical mechanics analogue constants used in cases 1-7, with the largest deviations occurring for  $H_2$  and hydrides (21, , p. 109). For example, the differences between the molecular constants of  $H_2 X 1s\sigma$  state (taken from (34)) and the corresponding Dunham coefficients, obtained in this work, are 0.12% for  $\omega_e$  and  $Y_{10}$ , 3% for  $\omega_e x_e$  and  $Y_{20}$ , 72% for  $\omega_e y_e$  and  $Y_{30}$ , 0.015% for  $B_e$  and  $Y_{01}$ , 1.8% for  $\alpha_e$  and  $Y_{11}$ , 5.9% for  $\gamma_e$  and  $Y_{21}$ , 0.25% for  $D_e$  and  $Y_{02}$ , 40% for  $\beta_e$  and  $Y_{12}$ , etc. Dunham polynomial constants used together as a whole represent all experimental data more accurate than the classical picture in cases 1-7<sup>5</sup>. Results from Eq. (36) are then summed to obtain  $Q_{int}$ :

$$Q_{int} = \sum_{e,v,J}^{e_{max},v_{max},J_{max}} \omega_e(2J+1) \frac{1}{8} [(2S+1)^2 - (-1)^J(2S+1)] \exp\left[\frac{-c_2}{T} T_{Dun}\right]. \quad (37)$$

In this case,  $v_{max}$  and  $J_{max}$  are evaluated numerically, defined as the first  $v$  or  $J$ , where  $\Delta E \leq 0$  (as in case 2, but now based on less biased coefficients), with  $\Delta E$  given as

$$\Delta E(v) = \sum_{i=1}^{i_{max}} Y_{i,0} \left[ \left(v + \frac{3}{2}\right)^i - \left(v + \frac{1}{2}\right)^i \right] \leq 0, \quad (38)$$

for  $v_{max}$ , and

$$\Delta E(J) = \sum_{i=0,k=1}^{i_{max},k_{max}} Y_{i,k} \left(v + \frac{1}{2}\right)^i [(J+1)^k (J+2)^k - J^k (J+1)^k] \leq 0 \quad (39)$$

for  $J_{max}$ .

## 4. Thermodynamic properties

From  $Q_{tot}$  and its first and second derivatives we calculate thermodynamic properties. For  $Q_{tr}$  (Eq. (1)) we assume 1 mol of ideal-gas molecules,  $N = N_A$ , Avogadro's number. The ideal-gas standard-state pressure (SSP) is taken to be  $p^\circ = 1$  bar and the molecular mass is given in amu. The internal contribution  $E_{int}$  to the thermodynamic energy, the internal energy  $U - H(0)$ , the enthalpy  $H - H(0)$ , the entropy  $S$ , the constant-pressure specific heat  $C_p$ , the constant-volume specific heat  $C_v$ , the Gibbs free energy  $G - H(0)$ , and the adiabatic index  $\gamma$  are obtained respectively from

$$E_{int} = RT^2 \frac{\partial \ln Q_{int}}{\partial T} \quad (40)$$

$$U - H(0) = E_{int} + \frac{3}{2} RT \quad (41)$$

$$H - H(0) = E_{int} + \frac{5}{2} RT \quad (42)$$

<sup>5</sup> In most cases the estimated energies from Dunham polynomials differ by less than  $1 \text{ cm}^{-1}$  from experimentally determined energies. For high energies they can, however, sometimes differ by up to  $20 \text{ cm}^{-1}$ .

$$S = R \ln Q_{tot} + \frac{RT}{Q_{tot}} \left( \frac{\partial Q_{tot}}{\partial T} \right) \quad (43)$$

$$C_p = R \left[ 2T \left( \frac{\partial \ln Q_{int}}{\partial T} \right) + T^2 \left( \frac{\partial^2 \ln Q_{int}}{\partial T^2} \right) \right] + \frac{5}{2}R \quad (44)$$

$$C_v = \frac{\partial E_{int}}{\partial T} + \frac{3}{2}R \quad (45)$$

$$G - H(0) = -RT \ln Q_{tot} + RT \quad (46)$$

$$\gamma = \frac{H - H(0)}{U - H(0)}. \quad (47)$$

## 5. Orto/para ratio of molecular hydrogen

In addition to equilibrium hydrogen, we also calculate the normal hydrogen following the paradigm of (9). In this case, ortho-hydrogen and para-hydrogen are not in equilibrium, but act as separate species. This aspect is particularly important for simulations of protoplanetary disks. The equilibrium timescale is short enough (300 yr) that the ortho/para ratio (OPR) can thermalise in the lifetime of a disk, but the equilibrium timescale is longer than the dynamical timescale inside about 40 AU (5). In case of normal hydrogen, ortho and para states have to be treated separately. Then Eq. (37) is split into two, one for para states:

$$Q_{para} = \sum_{e,v,J_{\text{even}}}^{e_{\text{max}},v_{\text{max}},J_{\text{max}}} \omega_e(2J+1) \exp \left[ \frac{-c_2}{T} T_{Dun} \right], \quad (48)$$

and one for ortho states:

$$Q_{ortho} = \sum_{e,v,J_{\text{odd}}}^{e_{\text{max}},v_{\text{max}},J_{\text{max}}} \omega_e(2J+1) \exp \left[ \frac{-c_2}{T} (T_{Dun} - \epsilon_{001}) \right]. \quad (49)$$

We note that weights for nuclear spin-split are omitted. The partition function for ortho-hydrogen is (as opposed to  $Q_{para}$ ) referred to the first excited rotational level ( $J = 1$ ) of the ground electronic state in its ground vibrational level.  $\epsilon_{001}$  can be considered as the formation energy of the ortho-hydrogen (9).  $Q_{int}$  is then (9)

$$Q_{int}^{norm} = (Q_{para})^{g_p} (Q_{ortho})^{g_o}, \quad (50)$$

where  $g_p$  and  $g_o$  are the statistical weights of the ortho and para configurations, 0.25 and 0.75, respectively. Moreover, the OPR is not necessarily either 3 or in equilibrium, but can be a time-dependant variable. The last consideration is beyond the scope of this work, therefore we do not discuss different ratios and assume that there are only two possibilities: either  $H_2$  is in equilibrium or not.

## 6. Results and comparison

We finally are ready to compare these different approaches. We here focus on  $H_2$ , but we plan to apply the theory given above to other molecules in a forthcoming paper. Since  $Q_{int}$  varies with several orders of magnitude as a function of temperature, we normalised the differences to case 8:  $\frac{Q_{tot,X} - Q_{tot,8}}{Q_{tot,8}}$ , where  $X$  is the case number.

Molecular constants for cases 1-7 were taken from the NIST<sup>6</sup> database, summarised in (34).  $D_0 = 36118.0696 \text{ cm}^{-1}$  (35). Experimental and theoretical data for molecular hydrogen for case 8 was taken from a number of sources that are summarised in Table 1. Theoretical calculations were used only when observational data were incomplete. For every electronic state, coefficients were fitted to all  $v - J$  configurations simultaneously using a weighted Levenberg-Marquardt (43) algorithm and giving lower weights to theoretical data.

### 6.1. Determination of Dunham coefficients and evaluation of their accuracy

In this subsection we show how estimated energies from our Dunham coefficients for particular  $e, v, J$  configurations compare to those estimated from molecular constants and to experimental data. For simplicity we will here discuss only two electronic ( $X 1s\sigma, D 3p\pi$ )<sup>7</sup> and vibrational ( $v = 0$  and 10) configurations of molecular hydrogen. Additionally, for the  $X 1s\sigma$  state we show Dunham coefficients from (10) and (25). For (10) signs had to be inverted for the  $Y_{02}, Y_{04}, Y_{12}, Y_{14}$ , and  $Y_{22}$  coefficients so that they would correctly follow the convention presented in Eq. (36). The comparison is shown in Fig. 2. The top panels show vibrational energies of both states, middle panels show energy levels of the  $v = 0$  vibrational state, and bottom panels show energy levels of the  $v = 10$  vibrational state. Experimental data are shown as black dots, red curves represent calculations of this work, green curves calculations from molecular constants, blue and cyan calculations using Dunham coefficients from (25) and (10), respectively. The top panels in all panels show the resulting energies, the bottom panels the residuals (calculated - experimental) in logarithmic scale. Triangles, facing down, indicate that the calculated energy is lower than observed, upward facing triangles that it is higher. These figures show that energies calculated from molecular constants can diverge substantially, especially in the  $X 1s\sigma$  state, which contributes most to  $Q_{int}$ . For most of the states the results of (25) are of similar quality as ours (but we used fewer coefficients, which speeds up the  $Q_{int}$  calculation), while for the lower vibrational levels of the  $X 1s\sigma$  state our results are much more accurate (especially at high  $J$ ). A complete set of Dunham coefficients is given in Tables 2 to 23 (available online). The number of coefficients for all cases was chosen separately from examining the RMSE (root mean square error, compared to experimental/theoretical data) to determine those with the lowest number of coefficients and lowest RMSE. In some cases as little as a 5x5 matrix is enough (e.g.  $EF 2p\sigma 2p\sigma^2$ ), whereas in other cases up to a 11x11 matrix

<sup>6</sup> K.P. Huber and G. Herzberg, "Constants of Diatomic Molecules" (data prepared by J.W. Gallagher and R.D. Johnson, III) in NIST Chemistry WebBook, NIST Standard Reference Database Number 69, Eds. P.J. Linstrom and W.G. Mallard, National Institute of Standards and Technology, Gaithersburg MD, 20899, <http://webbook.nist.gov>, (retrieved July 19, 2014).

<sup>7</sup> These states have a sufficiently large amount of molecular constants determined. Most other states have only few to no molecular constants determined, thus comparing them would be ungentlemanly.

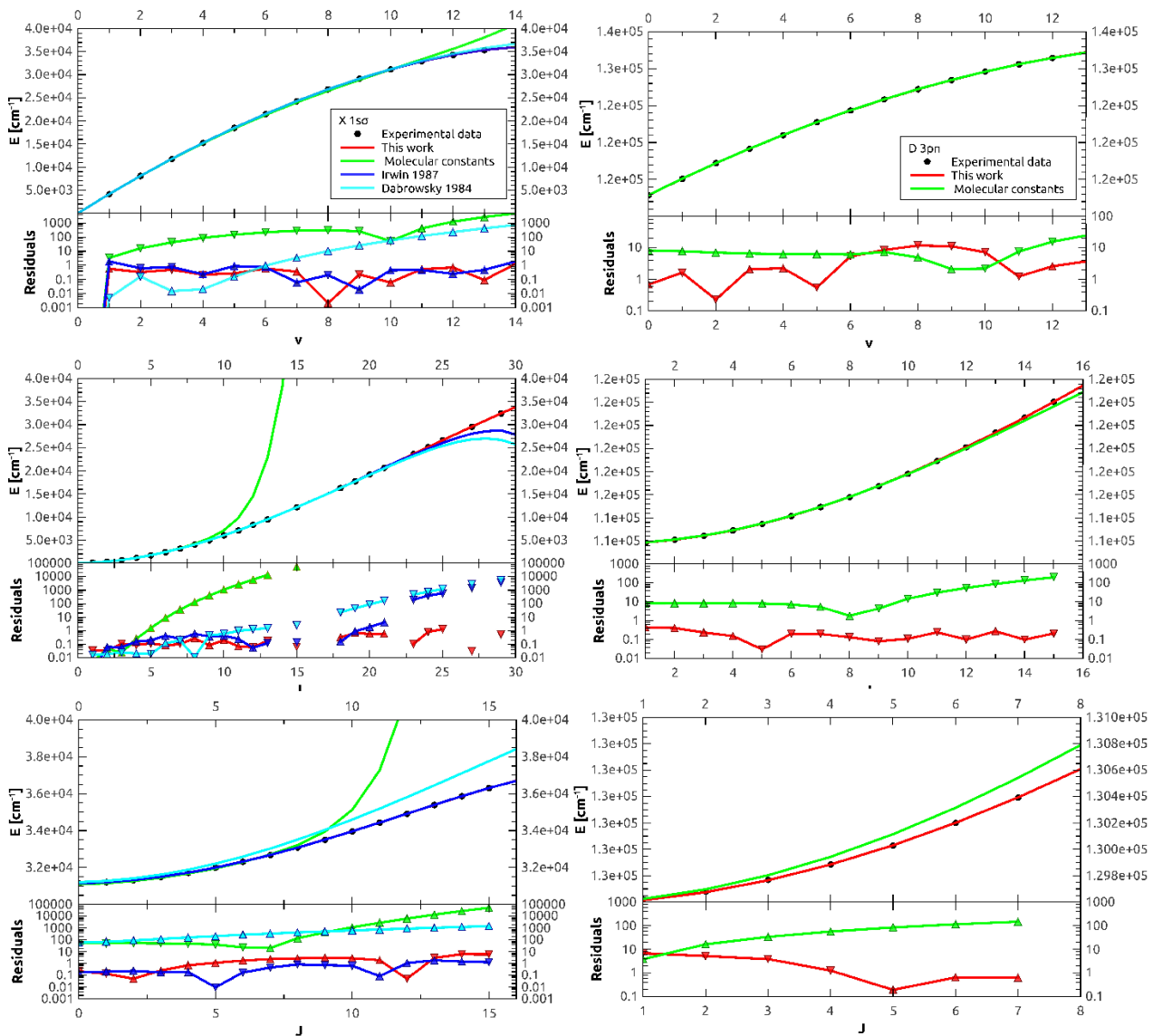


**Fig. 2.** Energy levels for the  $X\ 1\sigma$  and  $D\ 3p\pi$  states of  $H_2$ . Top left:  $X\ 1\sigma$  vibrational energies. Top right:  $D\ 3p\pi$  vibrational energies. Middle left:  $X\ 1\sigma$  ( $v = 0$ ) energy levels. Middle right:  $D\ 3p\pi$  ( $v = 0$ ) energy levels. Bottom left:  $X\ 1\sigma$  ( $v = 10$ ) energy levels. Bottom right:  $D\ 3p\pi$  ( $v = 10$ ) energy levels. See text for more details.

is needed. These differences depend on the complexity of the shape of the potential well. In all the tables the limiting energies are given up to which particular matrices should be used. All the limitations have to be employed (maximum energy as well as Eqs. (38) and (39)) for every electronic configuration, since all the coefficients are only valid under these limitations.

## 6.2. Comparison of cases 1 to 8

First, we consider only the equilibrium  $H_2$ . The comparison of cases 1-7 to case 8 is shown in Fig. (3). The main differences between all cases come from whether or not rigid-rotor approximation is used. The simplest case, case 1, underestimates  $Q_{int}$  throughout the complete temperature range. The underestimation in the high-temperature range is easily explained by the equidistant separation (or linear increase with increasing  $J$ ) between eigenstates (Eqs. (4) and (13), respectively): in HOA/RRA the eigenstate energies are higher for a given set of  $v$ ,  $J$  values than when less strict approximations are used (Eq. (7)). This ef-

fect is particularly strong for  $H_2$ , since the rotational distortion constant  $D_e$  (see Eq. (18)) is so large ( $D_{e,H_2} = 0.0471$  for the  $X^1\Sigma_g$  state, whereas it is only  $D_{e,CO} = 6.1215 \times 10^{-6}$  in the case of CO). The higher energy levels are therefore less populated in the HOA/RRA than in a more realistic computation, and these levels play a relatively larger role the higher the temperature. At the lowest temperatures the few lowest eigenstates dominate the value of  $Q_{int}$ , and these levels have slightly too high energies in HOA/RRA and therefore also cause  $Q_{int}$  from HOA/RRA to be substantially underestimated for low temperatures. Numerical differences are small, but the percentage difference is substantial: between 80 K and 1200 K the difference is 10 to 20 percent. Anharmonicity (difference between cases 1 and 2) for  $H_2$  is only relevant above 1000 K. Interaction between rotation and vibration gives only 2 percent difference (between cases 2 and 3) below 2000 K and becomes substantial thereafter. Since  $D_0 = 36118.0696\text{ cm}^{-1}$ , and  $T_e = 91700\text{ cm}^{-1}$  for the  $B^1\Sigma_u^+$  state, for  $H_2$  it makes no difference whether excited electronic states are taken into account or not for low temperatures or if



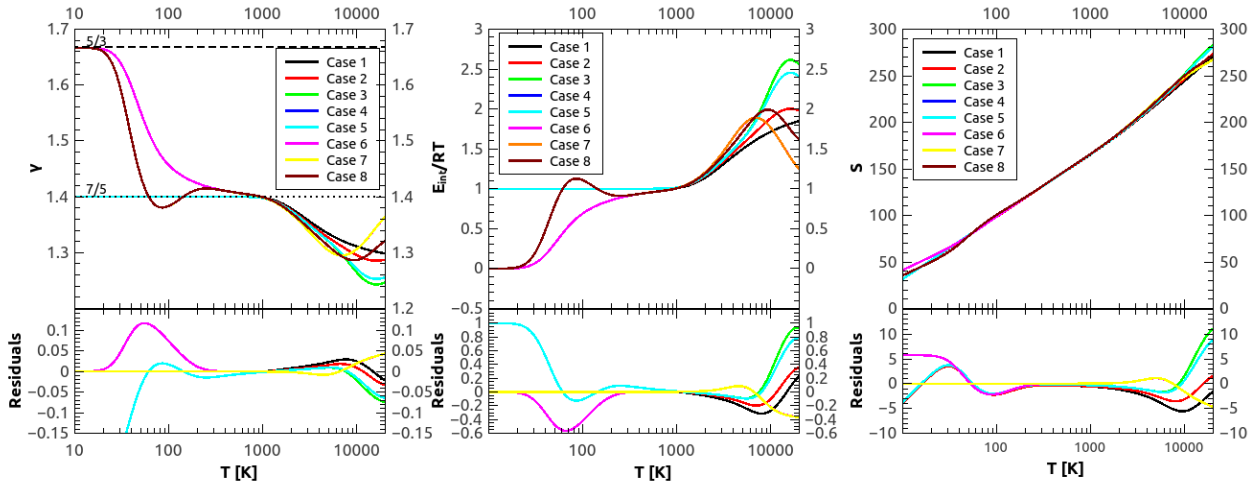


**Fig. 4.** Adiabatic index (left panel), normalised internal energy (middle panel), and entropy (right panel) for the  $\text{H}_2$  molecule. In the left panel we also show the constants  $\gamma = 5/3$  and  $\gamma = 7/5$ . Residuals are for cases 1-7 with respect to case 8. In the left panel cases 1-5 are equal to  $\gamma = 7/5$  below 1000 K, case 6 is identical to case 7 after 300 K, and case 7 is identical to case 8 until 6000 K; in the middle panel cases 1 to 5 are identical until 1000 K, and case 7 is almost identical to case 8 until 2000 K.

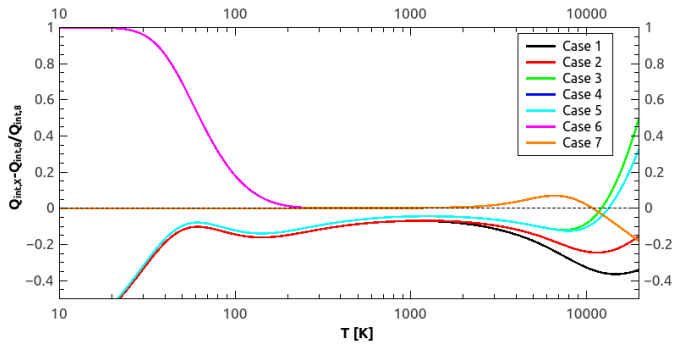


**Fig. 3.** Comparison of different approaches for calculating  $Q_{int}$  for the  $\text{H}_2$  molecule. Case 1 is identical to case 2 below 1500 K; case 4 is completely identical to case 5 for  $\text{H}_2$ . All of the methods (i.e. cases 1-7) diverge substantially from our most accurate computation (case 8) for low as well as high temperatures.

arbitrary truncation (e.g.  $40000 \text{ cm}^{-1}$ ) is below the first excited state. On the other hand, summing above the dissociation energy, at temperatures above 10000 K gives larger  $Q_{int}$  than it should be, assuming only the ground electronic state is available. On the other hand, if the RRA is used,  $Q_{int}$  is still somewhat too low even if erroneously, it is summed to infinity. Case 6 shows how large the difference is when nuclear spin-split degeneracy is omitted from the full calculations and  $\sigma = 1/2$  is used. For temperatures below 200 K, case 6 overestimates the partition function by up to a factor of 2 compared to case 8. For T between 200 K and 2000 K, cases 6 and 7 are indistinguishable from case 8. Above 2000 K even case 7 (and 6) gives different results. The latter is due to poor predictions of the higher rotational energy states at higher vibrational levels.

Naturally, using different approaches (cases 1-8) leads to different estimates of thermodynamic quantities. In Fig. 4 the adiabatic index  $\gamma$ , the normalised internal energy ( $E_{int}/RT$ ), and the entropy  $S$  are shown for all the cases. Constant adiabatic indexes ( $5/3$  or  $7/5$ ) clearly completely misrepresent reality for a wide range of temperatures when local thermal equilibrium (LTE) is assumed. When considering the simplest cases (case 1 to 5), they follow the  $7/5$  simplification well until 1000 K, but are far from

the most realistic estimate (case 8). Case 6 gives results almost identical to case 7 above 300 K. Case 7 is indistinguishable from case 8 up until 2000 K. The same trends can be seen for internal energy. From a first glance, the entropy seems to be very similar in all the cases, but this is because the dominating factor comes from  $Q_{tr}$ . Keeping that in mind, variability throughout all the temperature range is substantial. Entropy in case 7 is accurate until 3000 K.

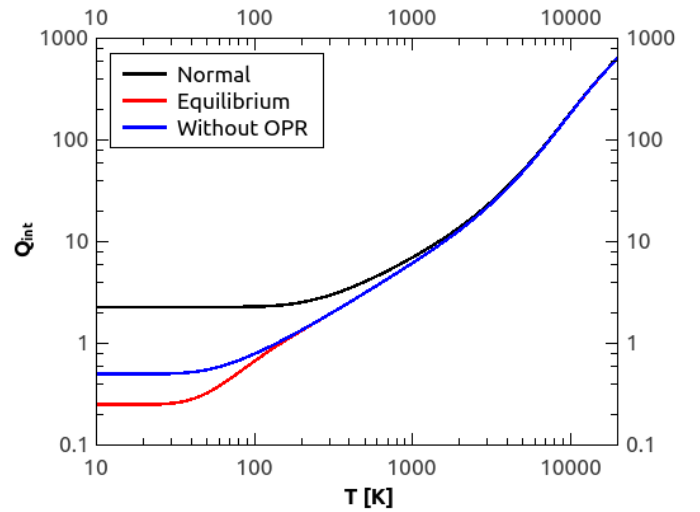


**Fig. 5.**  $Q_{int}$  for equilibrium, normal, and one (i.e. neglecting OPR) hydrogen.

Now we compare equilibrium and normal hydrogen. Equilibrium, normal, and one, neglecting OPR, partition functions are shown in Fig. (5). At low temperature, the three models show large differences, while in the high temperature range ( $T > 2000$  K) the results coalesce. The same trends can be seen for the calculated thermodynamic quantities (Fig. (6)). Both internal energy and specific heat at constant pressure are lower for normal hydrogen, whereas equilibrium hydrogen has higher values. The adiabatic index is dramatically different for both cases. Normal hydrogen does not have a depression at low temperatures. This depression can lead to accelerated gravitational instability and

collapse in molecular clouds to form pre-stellar cores and protoplanetary cores in protoplanetary disks. Large differences in entropy are only present at temperatures below 300 K. Neglecting OPR would lead to intermediate values between normal and equilibrium hydrogen.

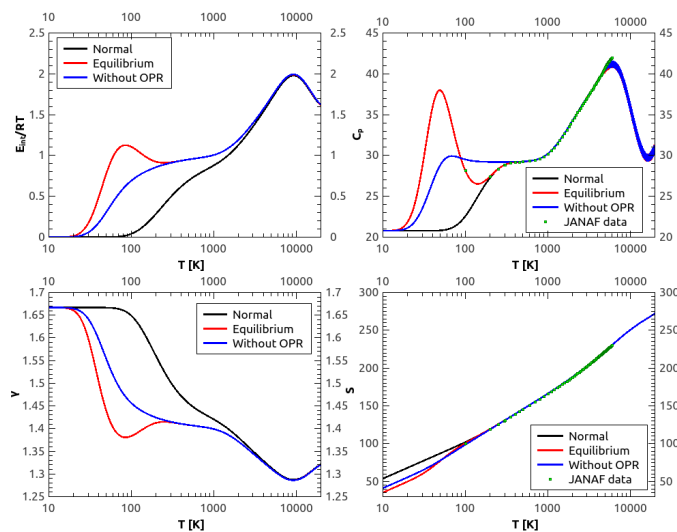


**Fig. 6.** Normalised internal energy,  $C_p$ , adiabatic index and entropy, calculated for equilibrium, normal, and with neglected OPR hydrogen. For  $C_p$  and entropy JANAF data are also shown.

### 6.2.1. Other studies.

There are a number of commonly used studies of  $Q_{int}$ . Here we give a brief summary of how other studies were performed, which simplifications they used, which molecular constants were adopted, and for which temperature range they were recommended. We stress that although it is commonly done, data must not be extrapolated beyond the recommended values under any circumstances. The resulting partition functions as well as their derivatives often diverge from the true values remarkably fast outside the range of the data they are based on. In our present study we took care to validate our data and formulas, such that they can be used in a wider temperature range than those of any previous study. Our data and formulas can be safely applied in the full temperature range from 1 K to 20000 K and easily extended beyond 20000 K in extreme cases, such as shocks, by use of the listed Dunham coefficients.

Tatum 1966 (42, T1966) presented partition functions and dissociation equilibrium constants for 14 diatomic molecules in the temperature range  $T = 1000 - 8000$  K with 100 K steps. Calculations were made using case 5. The upper energy cut-off was chosen to be at  $40000 \text{ cm}^{-1}$ . Only the first few molecular constants were used ( $\omega_e, \omega_e x_e, B_e, \alpha_e$ ).

Irwin 1981 (24, I1981) presented partition function approximations for 344 atomic and molecular species, valid for the temperature range  $T = 1000 - 16000$  K. Data for molecular partition functions were taken from (42; 31; 26). (24) gave partition function data in the form of polynomials,

$$\ln Q = \sum_{i=0}^5 a_i (\ln T)^i, \quad (51)$$

which is very convenient to use. For each species, the coefficients of Eq. (51) were found by the method of least-squares fitting. Some molecular data were linearly extrapolated before fitting the coefficients. For the extrapolated data the weight was reduced by a factor of  $10^6$ . Irwin stated that these least-squares fits have internally only small errors. However, a linear extrapolation to strongly non-linear data results in large errors even before fitting the polynomial, and the size of the errors due to this effect was not estimated.

Bohn and Wolf 1984 (4, BW1984) derived partition functions for  $\text{H}_2$  and  $\text{CO}$  that are valid for the temperature range  $T = 1000 - 6000$  K. In principle, this paper aimed to show a new approximate way of calculating partition functions, specific heat  $c_v$ , and internal energy  $E_{int}$ . Calculations were made using case 5 for "exact" partition functions and using assumptions of case 3 for approximations. Only the ground electronic state was included, and only the first few molecular constants were used ( $\omega_e, \omega_e x_e, B_e, \alpha_e$ ).

Sauval and Tatum 1984 (38, ST1984) presented total internal partition functions for 300 diatomic molecules, 69 neutral atoms, and 19 positive ions. Molecular constants ( $\omega_e, \omega_e x_e, B_e, \alpha_e$ ) were taken from (23). The partition function polynomial approximations are valid for the temperature range  $T = 1000 - 9000$  K. The authors adopted the previously used equation, [T1966] (case 5) for all the species. A polynomial expression

$$\log Q = \sum_{n=0}^4 a_n (\log \theta)^n \quad (52)$$

was used for both atoms and molecules. Here  $\theta = 5040/T$ .

Rossi et al. 1985 (37, R1985) presented total internal partition functions for 53 molecular species in the temperature range  $T = 1000 - 5000$  K. Molecular constants ( $\omega_e, \omega_e x_e, B_e, \alpha_e$ ) were taken from (23). For diatomic molecules the authors followed Tatum's (42) paradigm, case 5. The authors claimed that  $Q_J$  was evaluated with a non-rigid approximation (37), but upon a simple inspection it is clear that they used rigid-rotor approximation. They did, however, allow interaction between vibration and rotation. An arbitrary truncation in the summation over the electronic states is at  $40000 \text{ cm}^{-1}$ . For polynomial approximations the authors considered the "exact" specific heat, whose behaviour near the origin is more amenable to approximation schemes. The partition functions were then obtained by integration (37). Their specific heat approximation is

$$\frac{C_v}{k} = \sum_{m=0}^4 a_m Z^m, \quad (53)$$

where  $Z = T/1000$  and  $a_m$  are coefficients. The partition function they obtained is listed as the seven fitting constants  $a_0$  to  $a_6$  to the polynomial:

$$\ln Q = a_0 \ln Z + \sum_{m=1}^4 \frac{a_m}{m(m+1)} Z^m - \frac{a_5}{Z} + a_6. \quad (54)$$

Kurucz 1985 (28, K1985) commented on the situation regarding the partition functions of  $\text{H}_2$  and  $\text{CO}$ . Approximate expressions for the molecular partition functions in previous studies

were considered not rigorous enough because they did not include coefficients of sufficiently high order and did not keep proper track of the number of bound levels. K1985 used experimentally determined energy levels, when available, and supplemented them with fitted values, presumably extended to a higher cut-off energy as discussed in Sect. 2.6 and Fig. 1 above. The author explicitly summed over the energies of the three lowest electronic states (data for  $H_2$  were derived from (10)) and gave polynomial fits for the partition functions between 1000 K and 9000 K and also tabulated the exact results with steps of 100 K.

**Irwin1987 (25, I1987)** Irwin (1987) presented refined total internal partition functions for  $H_2$  and CO. The partition function polynomial approximations are valid for the temperature range  $T = 1000 - 9000$  K. Estimated errors at 4000 K are 2% for  $H_2$  and 0.004% for CO.  $Y_{i,j}$  for  $H_2$  were determined by using an equally weighted simultaneous least-squares fit of Dunham series using energy data obtained from (10). This was done for the ground  $H_2$  electronic state only.

I1987 compared his results with those of (28; 38) and found slightly higher values of  $Q$ , which he attributed to a combination of the number of included electronic states and a difference in the treatments of the highest rotational levels. Our results indicate that the main difference between the results of I1987(25) and K1985(28) is the use of slightly too low energies in I1987 of the highest rotational levels, and we conclude that the value trend by K1985 is slightly closer to the values obtained by a full treatment (our case 8) than are those of I1987. A main difference between our method and those of I1987, K1985, and older works is, however, that our method is applicable in a higher temperature range and can treat ortho and para states separately. It can therefore be used in a wider range of physical conditions, including shocks, non-equilibrium gasses, etc.

**Pagano et al. 2009(34, P2009)** presented internal partition functions and thermodynamic properties of high-temperature (50 - 50000 K) Jupiter-atmosphere species. The authors used case 7 to calculate the partition functions with more than the first few (e.g.  $\omega_e$  and  $\omega_e x_e$ ,  $B_e$  and  $D_e$ ) molecular constants for the ground and first few electronically excited states. The calculations are completely self-consistent in terms of maximum rotational states for the individual vibrational levels, presumably such that  $E(v, J_{\max}) \approx D_0$  for each  $v$ .

**Laraia et al. 2011 (29, L2011)** presented total internal partition functions for a number of molecules and their isotopes for the temperature range 70 - 3000 K. The methods used in this study are based on (14; 12). Rotational partition functions were determined using the formulae in (32; 33). Vibrational partition functions were calculated using the harmonic oscillator approximation of (22). All state-dependent and state-independent degeneracy factors were taken into account in this study. The  $H_2$  partition function was calculated as a direct sum using ab initio energies. A four-point Lagrange interpolation was used for the temperature range with intervals of 25 K. Data are presented in an easily retrievable FORTRAN program (29).

**Colonna et al. 2012(9, C2012)** gave a statistical thermodynamic description of  $H_2$  molecules in normal ortho/para mixture. The authors determined the internal partition function for normal hydrogen on a rigorous basis, solving the existing ambi-

guity in the definition of those quantities directly related to partition functions rather than on its derivatives (9). The authors used case 7 with more molecular constants for the ground and first few electronically excited states than shown with equations 35. Internal partition function as well as thermodynamic properties for 5 - 10000 K are also given.

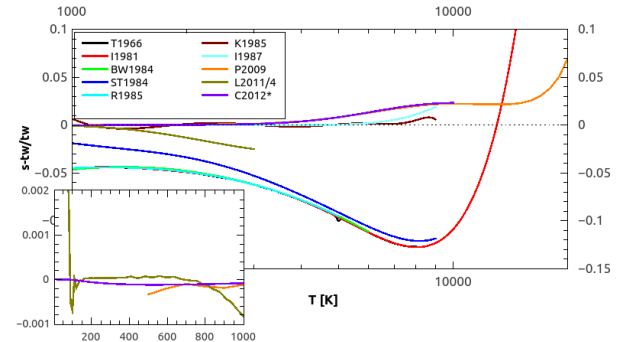


**Fig. 7.** Normalised  $Q_{int}$  from other studies in their respective temperature ranges. Normalisation is made with respect to the results of this work,  $([study - this\ work]/this\ work)$ . C2012 is normalised to normal hydrogen, all other studies to equilibrium hydrogen. The inset shows the low-temperature range.

**Comparison.** Figure 7 shows the normalised value of  $Q_{int}$  for molecular hydrogen from the ten different studies we have described here, in their respective temperature ranges listed in the respective studies. The normalisation is made with respect to the results of this work (case 8). For C2012 normal hydrogen  $Q_{int}$  is used, whereas equilibrium hydrogen  $Q_{int}$  is used for all the other studies. The main frame of Fig. 7 is for the 1000-20000K temperature range. The inset shows the low-temperature (10 - 1000 K) range. In the low-temperature range our results clearly differ only marginally from the three studies (P2009, L2011, C2012) that listed values of  $Q_{int}$  for low temperatures (the percentage difference is smaller than 0.1 percent in most of the temperature range). Since L2011 did not normalise the spin-split degeneracy, their results had to be divided by a factor of 4 before the comparison, shown in Fig. 7. In the high-temperature range, all studies using cases 1-5 have large errors (also seen from our case comparison in Fig. 3). Since K1985 explicitly derived his partition functions from experimental energy data, his results are in very good agreement with our results (from case 8) for his given temperature range (1000 - 9000 K). I1987 is also in great agreement with both K1985 and our results for the same temperature range. Using the values of  $Y_{ij}$  determined by I1987 gives results that perfectly agree with our work, as expected. At the higher end of the I1987 recommended temperature range, however, the polynomial approximation starts to have larger errors (the estimated 2 percent). At the highest temperature range, P2009 and C2012 also start to show considerable errors. These two studies are the only ones based on summation of energy levels, calculated based on molecular constants, and the comparison of our work with P2009 and C2012 therefore illustrates approximately how large errors in  $Q_{int}$  are obtained from methods based on molecular constants. The reason is, as mentioned before, that molecular constants are commonly fitted to the bottom of the potential well and poorly represent higher vibrational and rotational states energies. Finally, the I1981 results follow the T1966 results perfectly until 8000 K, which is the latter's high temperature limit. Then, since I1981 extrapolated data, the corre-

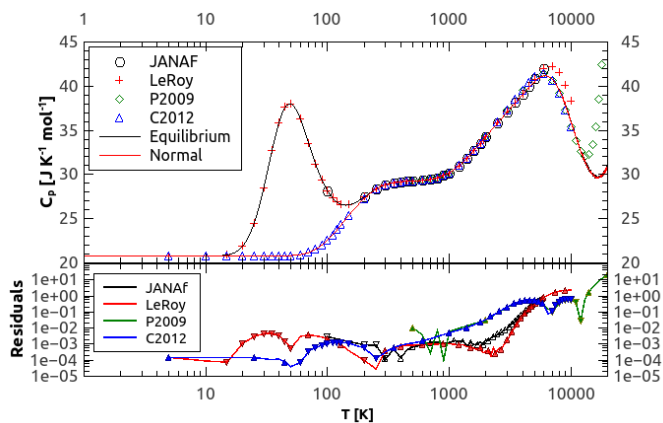


**Fig. 8.** Calculated  $C_p$  comparison to other studies. The top panel shows resulting  $C_p$  values, the bottom panel residuals (other - ours) on a logarithmic scale. Facing down triangles indicate that other results have lower values than ours, facing up triangles indicate that the values are higher.

sponding  $Q_{int}$  begin to show exponentially larger errors and is completely unreliable, which illustrates both how poor the HO + RR approximation represents reality (T1966 and I1981), and, in particular, how unreliable it can be to extrapolate beyond the calculated or measured data (as was done in the work of I1981), as seen clearly in Fig 7.

In Fig. 8 our results for  $H_2$  specific heat at constant pressure are compared to (26, JANAF), (30, LeRoy), (34, P2009) and (9, C2012). The latter is compared to our results for normal hydrogen, and the others are compared to our equilibrium hydrogen calculations. All calculations agree very well until 10000 K. Figure 9 depicts our results for entropy calculations for  $H_2$ . Once again, the agreement is very good (except with C2012 below 100 K), especially between our results and the JANAF data. However, there is a systematic offset between LeRoy and our results (and those of JANAF) of  $11.52 \text{ J K}^{-1} \text{ mol}^{-1}$ . This might be due to slightly different STP values, used by (30), resulting in slightly different  $Q_{tr}$ . We note that the JANAF data represent equilibrium  $H_2$ , while we computed equilibrium as well as normal and ortho and para  $H_2$  (and span a much wider temperature range), which makes our data more generally applicable.

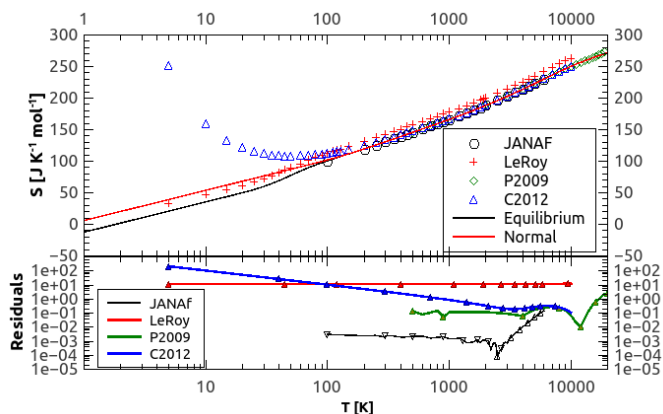


**Fig. 9.** Same as in Fig. 8, but for  $S$ .

### 6.3. Polynomial fits

Following the common practice, we present polynomial fits to our results. All partition function data were fit to a fifth-order polynomial of the form

$$Q_{int}(T) = \sum_{i=0}^5 a_i T^i. \quad (55)$$

The data for the partition function were spliced into three intervals to reach better accuracy. Polynomial constants are given in Table 24, and the fitting accuracy is shown in Fig. 10. Combining the three intervals, we reach an error smaller than 2 percent for all the temperature range. The decision for using lookup tables with significantly larger accuracy or the faster polynomial fits with increased errors needs to be made on an individual basis.

## 7. Conclusions

We have investigated the shortcomings of various simplifications that are used to calculate  $Q_{int}$  and applied our analyses to calculate the time-independent partition function of normal, ortho and para, and equilibrium molecular hydrogen. We also calculated  $E_{int}/RT$ ,  $H - H(0)$ ,  $S$ ,  $C_p$ ,  $C_v$ ,  $-[G - H(0)]/T$ , and  $\gamma$ . Our calculated values of thermodynamic properties for ortho and para, equilibrium, and normal  $H_2$  are presented in Tables 26, 25, 27, and 28, rounded to three significant digits. Full datasets in 1 K temperature steps<sup>8</sup> can be retrieved online from (47). The partition functions and thermodynamic data presented in this work are more accurate than previously available data from the literature and cover a more complete temperature range than any previous study in the literature. Determined Dunham coefficients for a number of electronic states of  $H_2$  are also reported.

In future work we plan to use the method we described here to calculate partition functions and thermodynamic quantities for other astrophysically important molecular species as well.

*Acknowledgements.* We thank Åke Nordlund and Tommaso Grassi for a critical reading of this manuscript and all the very valuable discussions. We are also grateful to the referee, Robert Kurucz, for valuable comments and suggestions. AP work is supported by grant number 1323-00199A from the Danish Council for Independent Research (FNU).

## References

- [1] Abgrall, H., Roueff, E., Launay, F., Roncin, J. Y., & Subtil, J. L. 1993, *Journal of Molecular Spectroscopy*, 157, 512
- [2] Abgrall, H., Roueff, E., Launay, F., & Roncin, J.-Y. 1994, *Canadian Journal of Physics*, 72, 856
- [3] Bailly, D., Salumbides, E. J., Vervloet, M., & Ubachs, W. 2010, *Molecular Physics*, 108, 827
- [4] Bohn, H. U., & Wolf, B. E. 1984, *Astronomy & Astrophysics*, 130, 202
- [5] Boley, A. C., Hartquist, T. W., Durisen, R. H., & Michael, S. 2007, *Astrophysical Journal Letters*, 656, L89
- [6] Born, M., & Oppenheimer, R. 1927, *Annalen der Physik*, 389, 457
- [7] Cardona, O., Simonneau, E., & Crivellari, L. 2005, *Revista Mexicana de Fisica*, 51, 476
- [8] Cardona, O. & Corona-Galindo, M. G., 2012, *Revista Mexicana de Fisica*, 58, 174-179
- [9] Colonna G., D'Angola A. & Capitelli M., 2012, *International Journal of Hydrogen Energy*, 37, 12, 9656-9668
- [10] Dabrowski, I. 1984, *Canadian Journal of Physics*, 62, 1639
- [11] Dunham, J. L. 1932, *Physical Review*, 41, 721
- [12] Fischer, J., Gamache, R. R., Goldman, A., Rothman, L. S., & Perrin, A. 2003, *J. Quant. Spec. Radiat. Transf.*, 82, 401

<sup>8</sup> Data with smaller temperature steps or beyond the given temperature range can be requested personally from the corresponding author

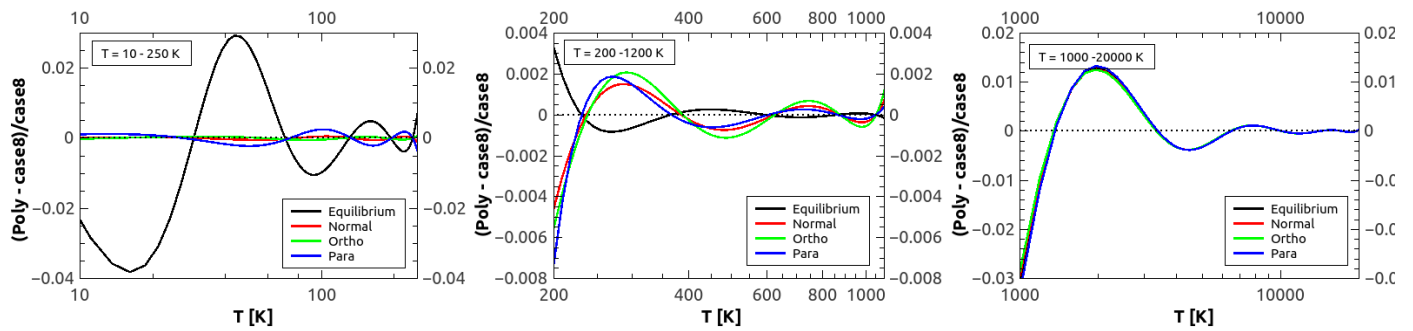


Fig. 10. Accuracies of polynomial fits for the partition functions of  $H_2$ .

- [13] Gamache, R. R., Hawkins, R. L., & Rothman, L. S. 1990, *Journal of Molecular Spectroscopy*, 142, 205
- [14] Gamache, R. R., Kennedy, S., Hawkins, R. L., & Rothman, L. S. 2000, *Journal of Molecular Structure*, 517, 407
- [15] Glass-Maujean, M., Klumpp, S., Werner, L., Ehresmann, A., & Schmoranzer, H. 2007, *J. Chem. Phys.*, 126, 144303
- [16] Glass-Maujean, M., & Jungen, C. 2009, *Journal of Physical Chemistry A*, 113, 13124
- [17] Glass-Maujean, M., Jungen, C., Schmoranzer, H., et al. 2013, *Journal of Molecular Spectroscopy*, 293, 19
- [18] Glass-Maujean, M., Jungen, C., Spielfiedel, A., et al. 2013, *Journal of Molecular Spectroscopy*, 293, 1
- [19] Glass-Maujean, M., Jungen, C., Schmoranzer, H., et al. 2013, *Journal of Molecular Spectroscopy*, 293, 11
- [20] Goorvitch, D. 1994, *ApJS*, 95, 535
- [21] Herzberg, G. 1950, "Molecular Spectra and Molecular Structure. Volume I: Spectra of Diatomic Molecules", New York: Van Nostrand Reinhold, 1950, 2nd ed.
- [22] Herzberg, J. G. 1960, "Molecular Spectra and Molecular Structure, II, Infrared and Raman Spectra of Polyatomic Molecules New York: Van Nostrand Reinhold, 1960, 2nd ed.
- [23] Huber, K. P. & Herzberg, J. G. 1979, New York: Van Nostrand Reinhold, 1979, ISBN 978-1-4757-0963-6
- [24] Irwin, A. W. 1981, *ApJS*, 45, 621
- [25] Irwin, A. W. 1987, *A&A*, 182, 348
- [26] Stull, D. R. & Prophet, H. 1971, U.S. Department of Commerce, 1971, vol. 2, NSRDS-NBS 37
- [27] Jørgensen, U. G., Almløf, J., Gustafsson, B., Larsson, M., Siegbahn, P. 1985, *J. Chem. Phys.*, 83, 3034-3041
- [28] Kurucz, R. L. 1985, Private communication, July 2014
- [29] Laraia, A. L., Gamache, R. R., Lamouroux, J., Gordon, I. E., & Rothman, L. S. 2011, *Icarus*, 215, 391
- [30] Le Roy, R. & Chapman, S. G., & McCourt, F. R. W. 1990, *The Journal of Physical Chemistry*, 94, 2
- [31] McBride, B. J., Heibel, S., Ehlers, J. G., & Gordon, S. 1963, NASA Special Publication, 3001,
- [32] McDowell, R. S. 1988, *J. Chem. Phys.*, 88, 356
- [33] McDowell, R. S. 1990, *J. Chem. Phys.*, 93, 2801
- [34] Pagano, D., Casavola, A., Pietanza, L. D., et al. 2009, *ESA Scientific Technical Review*, 257,
- [35] Piszczatowski, K., Łach, G., Przybytek, M., et al. 2009, *Journal of Chemical Theory and Computation*, 5, 11
- [36] Ross, S. C., & Jungen, C. 1994, *Phys. Rev. A*, 50, 4618
- [37] Rossi, S. C. F., Maciel, W. J., & Benevides-Soares, P. 1985, *A&A*, 148, 93
- [38] Sauval, A. J., & Tatum, J. B. 1984, *ApJS*, 56, 193
- [39] Senn, P., & Dressler, K. 1987, *J. Chem. Phys.*, 87, 6908
- [40] Sørensen, G. O. and Jørgensen, U. G., 1993, *J. Chem. Phys.*, 99, 3153
- [41] Takezawa, S. 1970, *J. Chem. Phys.*, 52, 2575
- [42] Tatum, J. B. 1966, *Publications of the Dominion Astrophysical Observatory Victoria*, 13, 1
- [43] Transtrum, M. K., & Sethna, J. P. 2012, arXiv:1201.5885
- [44] Vardya, M. S., 1965, *MNRAS*, 129, 345
- [45] Wólniewicz, L., Orlikowski, T., & Staszewska, G. 2006, *Journal of Molecular Spectroscopy*, 238, 118
- [46] Yu, S., & Dressler, K. 1994, *J. Chem. Phys.*, 101, 7692
- [47] [http://astro.ku.dk/~hpg688/thermodynamic\\_data.html](http://astro.ku.dk/~hpg688/thermodynamic_data.html)

**Table 1.** Summary of data sources for  $H_2$  energy levels

State	Experimental (levels)	Theoretical (levels)
$X\ 1s\sigma$	(10),(v = 0 – 14, J = 0 – 29)	
$B\ 2p\sigma$	(10),(v = 0 – 17, J = 0 – 30) (1), (v = 0 – 33, J = 0 – 28) (3), (v = 0 – 13, J = 0 – 13)	(45), (v = 0 – 38, J = 0 – 10)
$C\ 2p\pi$	(10),(v = 0 – 13, J = 1 – 13) (1), (v = 0 – 13, J = 1 – 24) (3), (v = 0 – 3, J = 0 – 7)	(45), (v = 0 – 13, J = 1 – 10)
$EF^{[a]}\ 2p\sigma 2p\sigma^2$	(39),(v = 0 – 20, J = 0 – 5) (3), (v = 0 – 28, J = 0 – 13)	(36), (v = 0 – 28, J = 0 – 5)
$B'\ 3p\sigma$	(2), (v = 0 – 7, J = 0 – 12) (3), (v = 0 – 3, J = 0 – 7)	(45), (v = 0 – 9, J = 0 – 10)
$D\ 3p\pi$	(2), (v = 0 – 14, J = 1 – 17) (3), (v = 0 – 2, J = 1 – 7)	(45), (v = 0 – 17, J = 1 – 10)
$GK^{[a]}\ 3d\sigma$	(3), (v = 0 – 6, J = 0 – 9)	(36), (v = 0 – 5, J = 0 – 5) (46) (v = 0 – 8, J = 0 – 5)
$H\bar{H}^{[a]}\ 3s\sigma$	(3), (v = 0 – 2, J = 0 – 6)	
$I\ 3d\pi$	(3), (v = 0 – 3, J = 1 – 10)	
$J\ 3d\delta$	(3), (v = 0 – 2, J = 2 – 6)	
$B''Bbar^{[a]}\ 4p\sigma$	(15),(v = 4 – 11, J = 0 – 2)	(45), (v = 0 – 56 <sup>[b]</sup> , J = 0 – 10) (15),(v = 4 – 11, J = 0 – 2)
$D'\ 4p\pi$	(41), (v = 0 – 5, J = 1 – 5)	(45), (v = 0 – 9, J = 1 – 10) (16),(v = 0 – 17, J = 1 – 4)
$5p\sigma$	(41), (v = 0 – 2, J = 0 – 4)	(45), (v = 0 – 9, J = 0 – 10) (17),(v = 0 – 8, J = 0 – 4)
$D''\ 5p\pi$	(41), (v = 0 – 2, J = 1 – 3) (18),(v = 0 – 12, J = 1 – 4)	(18),(v = 0 – 12, J = 1 – 4)
$6p\sigma$	(41), (v = 0 – 2, J = 0 – 4)	(45), (v = 0 – 9, J = 0 – 10) (17),(v = 0 – 7, J = 0 – 4)
$6p\pi$	(19),(v = 0 – 9, J = 1 – 4)	
$7p\sigma$	(41), (v = 0 – 2, J = 0 – 3)	(17),(v = 0 – 6, J = 0 – 4)
$7p\pi$	(19),(v = 0 – 7, J = 1 – 4)	

**Notes.** <sup>[a]</sup>Double potential well state. <sup>[b]</sup>32 lowest v levels are used in this study.

**Table 24.** Polynomial fit constants for partition functions of equilibrium, normal, and ortho and para  $H_2$ 

Low temperature (T = 10 - 250 K)						
Flavor	$a_0$	$a_1$	$a_2$	$a_3$	$a_4$	RMS
Equilibrium	2.673071615415136e-01	-3.495586051757211e-03	1.227901619954258e-04	-5.776440695273789e-07	9.251224490175610e-10	0.00516
Normal	2.277668085144430	3.115475456535298e-04	-1.199204285095701e-05	1.348313176588763e-07	-2.493525433376579e-10	0.00091
Ortho	2.996425936476927	3.807856081411796e-04	-8.659737634951350e-06	5.779158662343921e-08	-5.407749218414769e-11	0.00107
Para	9.994339093261912e-01	3.135419941617079e-04	-1.599408560500201e-05	2.032015813340736e-07	-4.090066248229891e-10	0.00186
Medium temperature (T = 200 - 1100 K)						
Flavor	$a_0$	$a_1$	$a_2$	$a_3$	$a_4$	RMS
Equilibrium	1.410033600294133e-01	6.085738724141971e-03	-4.096994909866605e-07	4.220221708082499e-10	-8.790594164685680e-14	0.0007
Normal	1.919800108599199	1.746213811668277e-03	7.693197369847348e-06	-6.504303232753276e-09	2.132168610356154e-12	0.00247
Ortho	2.891845114721733	-1.243647561012797e-03	1.312997140340565e-05	-1.105110818469195e-08	3.562652399419052e-12	0.00402
Para	3.312881928317837e-01	4.871438707876421e-03	2.339907793941012e-06	-2.214128676054798e-09	8.210809799374644e-13	0.00164
High temperature (T = 1000 - 20000 K)						
Flavor	$a_0$	$a_1$	$a_2$	$a_3$	$a_4$	RMS
Equilibrium	-9.661842638994980e-01	7.302127874247883e-03	-6.760893004505151e-07	3.128741080316710e-10	-1.645206030945910e-14	0.099
Normal	-1.142827289681385e-01	7.245357485089481e-03	-6.404547049175155e-07	3.110974834335349e-10	-1.642844436813594e-14	0.10151
Ortho	2.231696541394133e-01	7.190413006059544e-03	-6.192076726407582e-07	3.096074912455146e-10	-1.640036910200170e-14	0.10242
Para	-1.019053774741465e+00	7.360074236377774e-03	-6.935790834485644e-07	3.145274660505019e-10	-1.646581413255403e-14	0.10004
	$a_5$					
	2.788597060472472e-19					
	2.790315674249059e-19					
	2.790310846593324e-19					
	2.782419680521890e-19					

**Table 2.**  $Y_{i,j}$  for  $X$   $1s\sigma$  state.  $E_{max} = E_D = 36118.0696$ .

$i \setminus j$	0	1	2	3	4	5	6
0	0.0	60.8994	-0.0464547	4.6066e-5	-4.44761e-8	2.89037e-11	-8.51258e-15
1	4408.97	-3.22767	0.00251022	-2.85502e-6	2.15163e-9	-7.60784e-13	
2	-127.648	0.165697	-0.000458971	5.036e-7	-2.1465e-10		
3	2.90163	-0.031327	6.61024e-5	-4.15522e-8			
4	-0.302736	0.00278106	-3.45438e-6				
5	0.0175198	-0.000105554					
6	-0.000606749						

**Table 3.**  $Y_{i,j}$  for  $B$   $2p\sigma$  state.  $E_{max} = 118376.981$ .

$i \setminus j$	0	1	2	3	4	5	6	7
0	89540.7	20.3249	-0.0244189	6.10056e-5	-1.18524e-7	1.20211e-10	-4.73402e-14	2.11275e-20
1	1323.2	-1.09933	0.00881566	-4.47483e-5	1.02297e-7	-1.06706e-10	4.16538e-14	-1.58919e-19
2	1.11679	-0.153064	-0.000546492	6.67274e-6	-1.75266e-8	1.8647e-11	-7.16464e-15	4.0682e-20
3	-4.13726	0.063354	-0.000205483	7.37966e-8	4.55652e-10	-6.51076e-13	2.62926e-16	-2.00198e-21
4	0.394415	-0.0062084	2.25521e-5	-2.5732e-8	1.48268e-12	2.0649e-14	-1.16798e-17	
5	-0.0155583	0.000194542	-5.03613e-7	1.07722e-10	4.69293e-13	-4.60339e-16		
6	8.69305e-5	3.59161e-6	-2.00997e-8	3.79657e-11	-1.75735e-14			
7	1.09635e-5	-3.72309e-7	9.95017e-10	-7.35739e-13				
8	-2.49984e-7	8.41556e-9	-1.11877e-11					
9	-6.45466e-11	-6.35193e-11						
10	3.13732e-11							

$i \setminus j$	8	9	10
0	-2.50566e-19	-2.92577e-19	1.61127e-19
1	7.7568e-20	2.10342e-20	
2	-2.63039e-21		

**Table 4.**  $Y_{i,j}$  for  $C$   $2p\pi$  state.  $E_{max} = 118376.981$ .

$i \setminus j$	0	1	2	3	4	5	6	7
0	97882.0	32.5557	-0.0399421	0.000132418	-3.34989e-7	4.2892e-10	-2.12309e-13	3.53673e-19
1	2446.06	-3.09621	0.0222126	-0.000114815	2.84875e-7	-3.3416e-10	1.48677e-13	-1.64883e-19
2	-68.1303	0.685829	-0.00833825	3.73323e-5	-7.62593e-8	7.06128e-11	-2.30836e-14	
3	-0.0313063	-0.150771	0.00152702	-5.22981e-6	7.37665e-9	-3.65104e-12		
4	0.0746035	0.019201	-0.000146625	3.3335e-7	-2.36923e-10			
5	0.00144141	-0.00146403	7.19968e-6	-8.04132e-9				
6	-0.00185288	6.26612e-5	-1.45669e-7					
7	0.000162238	-1.20807e-6						
8	-4.75062e-6							

$i \setminus j$	8
0	-1.42451e-20

**Table 5.**  $Y_{i,j}$  for  $EF$   $2p\sigma 2p\sigma^2$  state, inner well.  $E_{max} = 105000.0$ .

$i \setminus j$	0	1	2	3	4
0	98068.8	23.2211	2.25688	-0.149909	0.00273895
1	2136.55	-8.10192	0.679069	-0.00863188	
2	140.173	-1.30784	-0.14758		
3	9.85717	1.4317			
4	-22.7252				

**Table 6.**  $Y_{i,j}$  for  $EF$   $2p\sigma 2p\sigma^2$  state, outer well.  $E_{max} = 118376.981$ .

$i \setminus j$	0	1	2	3	4	5	6
0	98606.2	5.74637	1.37059	-0.17094	0.00474712	0.000128489	-4.8543e-6
1	1454.02	-2.7411	-0.180194	0.022727	-0.00104196	1.65094e-5	
2	-80.3398	1.01425	0.00144103	-0.000222756	5.37232e-7		
3	1.77242	-0.101008	0.000235334	5.67045e-6			
4	0.191269	0.00388008	-9.85281e-6				
5	-0.0119227	-5.07168e-5					
6	0.000188356						

**Table 7.**  $Y_{i,j}$  for  $B'$   $3p\sigma$  state.  $E_{max} = 133610.273$ 

$i \setminus j$	0	1	2	3	4	5	6	7
0	109640.0	28.872	0.836305	-0.0136974	4.01261e-5	1.23323e-6	-1.6454e-8	8.27886e-11
1	1427.0	-15.3274	-2.85783	0.0525351	-0.000479745	2.55235e-6	-7.52893e-9	1.07135e-11
2	689.282	27.9589	2.41683	-0.0353017	0.000231187	-7.70384e-7	8.98726e-10	
3	-449.987	-22.3981	-0.880946	0.00944058	-3.7779e-5	6.29088e-8		
4	136.699	8.40707	0.160582	-0.00115863	2.0487e-6			
5	-21.732	-1.6006	-0.0142388	5.45786e-5				
6	1.61573	0.149031	0.000481531					
7	-0.0356702	-0.00537226						
8	-0.00077895							

$i \setminus j$	8
0	-1.55865e-13

**Table 8.**  $Y_{i,j}$  for  $D$   $3p\pi$  state.  $E_{max} = 133610.273$ .

$i \setminus j$	0	1	2	3	4	5	6	7
0	111713.0	30.0272	-0.0142088	-2.07092e-5	-5.35965e-8	1.77885e-9	-8.13272e-12	1.15704e-14
1	2354.63	-0.771873	-0.0151207	0.000144998	-7.04225e-7	1.31303e-9	1.27466e-12	-5.18074e-15
2	-68.7361	-0.431929	0.00809662	-6.33383e-5	2.90083e-7	-7.21926e-10	6.91788e-13	
3	2.91624	0.0927337	-0.00152849	8.35883e-6	-2.25164e-8	2.73782e-11		
4	-0.743664	-0.0073304	0.000130395	-4.7786e-7	5.34873e-10			
5	0.103972	8.18834e-5		1.01828e-8				
6	-0.00749572	1.39201e-5	6.07114e-8					
7	0.000262281	-4.49286e-7						
8	-3.56422e-6							
$i \setminus j$	8							
0	4.25363e-20							

**Table 9.**  $Y_{i,j}$  for  $GK$   $3d\sigma$  state, inner well.  $E_{max} = 116900.0$ .

$i \setminus j$	0	1	2	3	4
0	109217.0	23.8085	-0.253881	-0.00473545	1.98913e-5
1	970.614	-7.78821	0.412418	4.68762e-5	
2	24.2579	-1.06924	-0.0590925		
3	1.64268	0.369018			
4	-0.465966				

**Table 10.**  $Y_{i,j}$  for  $GK$   $3d\sigma$  state, outer well.

$i \setminus j$	0	1	2	3	4
0	110177.0	14.5226	0.387782	-0.0137014	0.000137787
1	1009.41	-7.16505	-0.0941763	0.00148123	
2	-25.2145	2.75273	0.00636093		
3	-1.88729	-0.245496			
4	0.489779				

**Table 11.**  $Y_{i,j}$  for  $H\bar{H}$   $3s\sigma$  state, inner well.  $E_{max} = 118000.0$ .

$i \setminus j$	0	1	2	3	4
0	111909.0	33.4756	-0.0628269	-0.00674187	8.95921e-5
1	2003.13	-12.1054	0.479189	0.00472823	
2	199.147	2.47998	-0.246944		
3	1.52825	0.64834			
4	-22.8763				

**Table 12.**  $Y_{i,j}$  for  $H\bar{H}$   $3s\sigma$  state, outer well.

$i \setminus j$	0	1	2	3	4	5	6
0	122617.0	2.85838	-0.452462	0.0496827	-0.00129124	-3.65898e-5	1.30097e-6
1	600.772	-2.03478	0.165172	-0.0186535	0.000900787	-1.33774e-5	
2	-178.292	0.705169	-0.0128	8.90067e-5	-7.25588e-6		
3	48.1293	-0.0969926	0.00148014	1.46566e-5			
4	-5.82021	0.00514187	-6.94023e-5				
5	0.319828	-8.17859e-5					
6	-0.00657088						

**Table 13.**  $Y_{i,j}$  for  $I$   $3d\pi$  state.

$i \setminus j$	0	1	2	3	4
0	110177.0	14.5226	0.387782	-0.0137014	0.000137787
1	1009.41	-7.16505	-0.0941763	0.00148123	
2	-25.2145	2.75273	0.00636093		
3	-1.88729	-0.245496			
4	0.489779				

**Table 14.**  $Y_{i,j}$  for  $J$   $3d\delta$  state.

$i \setminus j$	0	1	2	3
0	111260.0	41.8057	0.0950125	-0.00450042
1	2006.46	-6.68957	-0.0253833	
2	195.159	0.807222		
3	-56.9367			



**Table 15.**  $Y_{i,j}$  for  $B''Bbar$   $4p\sigma$  state, inner well.  $E_{max} = 130265.0$ .

$i \setminus j$	0	1	2	3	4	5	6
0	115722.0	116.926	-4.45735	0.188078	-0.00440882	4.63197e-5	-1.71816e-7
1	5867.53	-52.4159	-0.493037	0.0487225	-0.000747071	3.25362e-6	
2	-4015.06	44.4104	-0.526875	0.00647721	-2.37322e-5		
3	1961.35	-13.9427	0.00852245	-9.78352e-5			
4	-482.848	2.58965	0.000454106				
5	56.5459	-0.17409					
6	-2.50753						

**Table 16.**  $Y_{i,j}$  for  $B''Bbar$   $4p\sigma$  state, outer well.  $E_{max} = 138941.911$ .

$i \setminus j$	0	1	2	3	4	5	6
0	122624.0	0.95644	0.000305579	-3.2579e-6	-4.94167e-8	1.00874e-9	-4.52608e-12
1	360.513	0.00827397	-6.93853e-5	1.30952e-6	-1.07964e-8	3.57405e-11	
2	-4.41936	-0.00140404	1.00237e-6	-2.28296e-8	5.20907e-11		
3	0.0202615	6.54562e-5	5.32386e-8	2.54713e-10			
4	0.000542329	-1.81073e-6	-1.7598e-9				
5	-1.29422e-5	2.24736e-8					
6	8.5522e-8						

**Table 17.**  $Y_{i,j}$  for  $D'$   $4p\pi$  state.  $E_{max} = 138941.911$ .

$i \setminus j$	0	1	2	3	4	5	6
0	116682.0	30.2145	-0.0194539	-0.000248291	8.12785e-6	-8.99861e-8	3.37172e-10
1	2343.11	-1.70002	0.00414816	-8.34473e-5	9.02456e-7	-3.67685e-9	
2	-71.7393	0.0665521	0.000201895	-1.68829e-6	1.27848e-8		
3	2.55445	-0.0143264	-3.77337e-5	1.03224e-8			
4	-0.348338	0.00198268	2.02175e-6				
5	0.0287842	-0.000102487					
6	-0.000981186						

**Table 18.**  $Y_{i,j}$  for  $5p\sigma$  state.  $E_{max} = 143570.0$ .

$i \setminus j$	0	1	2	3	4	5	6
0	118948.0	12.553	-0.458717	-0.0753537	-0.00159359	9.37272e-5	9.54153e-6
1	1192.64	36.5609	3.12137	0.00958014	-0.00304086	-0.00015569	
2	956.798	-40.5327	-0.987989	0.015968	0.00140718		
3	-419.015	13.7138	0.0387677	-0.00421793			
4	83.7293	-1.72833	0.00539521				
5	-7.99491	0.072457					
6	0.288787						

**Table 19.**  $Y_{i,j}$  for  $5p\pi$  state.  $E_{max} = 143570.0$ .

$i \setminus j$	0	1	2	3	4	5	6
0	118995.0	36.0716	-0.319741	-0.014872	-0.000238203	1.99987e-5	2.23272e-6
1	2415.58	2.15448	0.505586	0.0148412	-0.000399269	-6.86912e-5	
2	-147.992	-7.47147	-0.160739	0.000242203	0.000546545		
3	36.0906	2.80197	0.00598473	-0.00176365			
4	-7.57518	-0.384299	0.0030262				
5	0.760411	0.016345					
6	-0.0284743						

**Table 20.**  $Y_{i,j}$  for  $6p\sigma$  state.  $E_{max} = 148240.0$ .

$i \setminus j$	0	1	2	3	4	5	6
0	120709.0	27.2762	-0.142997	0.00648973	0.000194723	-2.7412e-6	-6.47774e-7
1	61.5226	-15.6536	0.324584	0.00741685	-9.39748e-5	-1.86748e-5	
2	2379.78	7.34398	-0.0986585	0.00318703	-2.58488e-5		
3	-1170.3	-1.19031	-0.0159069	1.37776e-5			
4	269.026	0.074286	0.00197083				
5	-29.2007	-0.000671958					
6	1.20284						

**Table 21.**  $Y_{i,j}$  for  $6p\pi$  state.  $E_{max} = 148240.0$ .

$i \setminus j$	0	1	2	3	4	5	6
0	120320.0	58.0291	-0.686311	-0.0354304	-0.00063191	3.08385e-5	3.85789e-6
1	2264.49	-53.1853	1.41237	0.0776417	-1.83826e-5	-0.000191495	
2	15.0754	28.5592	-0.725983	-0.027318	0.00157845		
3	-37.0221	-6.48257	0.162007	-0.00265325			
4	7.77546	0.602542	-0.00483593				
5	-0.725696	-0.0217911					
6	0.0252225						

**Table 22.**  $Y_{i,j}$  for  $7p\sigma$  state.  $E_{max} = 150000.0$ .

$i \setminus j$	0	1	2	3	4	5	6
0	120984.0	14.4145	-0.206167	0.0189087	0.000577862	9.43236e-7	-1.05878e-6
1	2253.23	9.04999	0.299251	0.00127009	-0.000479448	-4.18786e-5	
2	-32.7638	-6.58075	-0.230493	0.00195881	0.000781566		
3	-8.66359	2.25858	0.021996	-0.00369885			
4	1.34773	-0.280184	0.00674419				
5	-0.16511	0.00597372					
6	0.0113496						

**Table 23.**  $Y_{i,j}$  for  $7p\pi$  state.  $E_{max} = 150000.0$ .

$i \setminus j$	0	1	2	3	4	5	6
0	121025.0	54.6852	-0.657303	-0.0278393	-0.000517054	1.93446e-5	2.61651e-6
1	2526.84	-33.3826	0.975964	0.0535573	0.000185217	-0.000113024	
2	-237.926	18.9794	-0.678591	-0.0232719	0.00118664		
3	63.6492	-4.60154	0.1826	-0.00237026			
4	-11.6711	0.422664	-0.00727658				
5	1.08902	-0.0152207					
6	-0.040398						

**Table 25.** Thermodynamic properties of equilibrium H<sub>2</sub>.

$T$ [K]	$Q_{int}$	$E_{int}/RT$ [J]	$H - H(0)$ [J mol <sup>-1</sup> ]	$S$ [J K <sup>-1</sup> mol <sup>-1</sup> ]	$C_p$ [J K <sup>-1</sup> mol <sup>-1</sup> ]	$C_v$ [J K <sup>-1</sup> mol <sup>-1</sup> ]	$-[G - H(0)]/T$ [J K <sup>-1</sup> mol <sup>-1</sup> ]	$\gamma$
5.0	0.25	0.0	103.931	21.095	20.786	0.0	-40.026	1.667
10.0	0.25	0.0	207.862	35.503	20.787	0.001	64.026	1.667
15.0	0.25	0.001	311.94	43.942	20.898	0.112	222.473	1.666
20.0	0.25	0.015	418.257	50.053	21.864	1.078	416.507	1.66
25.0	0.252	0.066	533.473	55.184	24.518	3.732	638.256	1.638
30.0	0.258	0.169	665.765	59.996	28.537	7.751	884.693	1.599
35.0	0.267	0.315	819.085	64.715	32.706	11.92	1154.933	1.551
40.0	0.282	0.48	991.15	69.305	35.893	15.107	1448.489	1.505
45.0	0.301	0.642	1175.533	73.647	37.61	16.824	1764.426	1.467
50.0	0.324	0.783	1364.975	77.638	37.97	17.184	2101.227	1.438
60.0	0.382	0.984	1737.824	84.441	36.242	15.456	2829.782	1.403
70.0	0.448	1.085	2086.766	89.826	33.537	12.75	3619.013	1.387
80.0	0.519	1.123	2409.737	94.142	31.153	10.367	4456.451	1.381
90.0	0.593	1.124	2711.881	97.703	29.377	8.591	5333.052	1.381
100.0	0.667	1.107	2999.115	100.73	28.151	7.365	6242.444	1.384
110.0	0.74	1.082	3276.322	103.373	27.351	6.565	7180.087	1.387
120.0	0.813	1.055	3547.19	105.73	26.867	6.081	8142.661	1.391
130.0	0.883	1.029	3814.429	107.869	26.613	5.827	9127.671	1.395
140.0	0.952	1.005	4080.006	109.837	26.526	5.739	10133.185	1.399
150.0	1.02	0.984	4345.331	111.668	26.556	5.77	11157.669	1.403
200.0	1.341	0.923	5692.821	119.414	27.448	6.662	16527.172	1.413
150.0	1.02	0.984	4345.331	111.668	26.556	5.77	11157.669	1.403
298.15	1.931	0.916	8467.176	130.682	28.836	8.05	28016.705	1.414
300.0	1.942	0.916	8520.534	130.86	28.849	8.063	28243.25	1.414
350.0	2.238	0.926	9969.563	135.327	29.081	8.294	34484.941	1.412
400.0	2.534	0.936	11426.436	139.218	29.181	8.395	40934.958	1.411
450.0	2.831	0.944	12886.795	142.658	29.229	8.442	47567.798	1.409
500.0	3.128	0.952	14349.02	145.739	29.259	8.473	54363.344	1.408
600.0	3.725	0.963	17278.057	151.079	29.326	8.54	68380.83	1.406
700.0	4.324	0.973	20215.836	155.608	29.44	8.654	82889.4	1.404
800.0	4.928	0.983	23168.335	159.55	29.623	8.837	97820.014	1.403
900.0	5.536	0.994	26142.864	163.053	29.88	9.094	113121.903	1.401
1000.0	6.151	1.006	29146.545	166.217	30.204	9.418	128756.479	1.399
1100.0	6.774	1.019	32185.337	169.113	30.579	9.793	144693.583	1.397
1200.0	7.406	1.034	35263.602	171.792	30.991	10.204	160909.037	1.395
1300.0	8.051	1.051	38384.094	174.289	31.421	10.635	177383.01	1.392
1400.0	8.709	1.069	41548.164	176.634	31.86	11.074	194098.888	1.389
1500.0	9.382	1.089	44756.054	178.847	32.297	11.511	211042.494	1.386
2000.0	13.015	1.193	61416.861	188.419	34.278	13.492	298792.538	1.371
2500.0	17.181	1.299	78962.143	196.243	35.838	15.052	390859.016	1.357
3000.0	21.964	1.397	97201.242	202.89	37.077	16.291	486526.148	1.345
3500.0	27.428	1.486	116007.0	208.686	38.121	17.335	585293.496	1.335
4000.0	33.632	1.568	135302.809	213.838	39.043	18.257	686790.762	1.326
4500.0	40.634	1.644	155031.8	218.484	39.852	19.066	790732.925	1.318
5000.0	48.492	1.713	175128.639	222.719	40.508	19.721	896892.151	1.311
6000.0	66.988	1.831	216042.905	230.176	41.156	20.37	1.115128382e6	1.3
7000.0	89.448	1.917	257096.393	236.506	40.779	19.993	1.340240895e6	1.293
8000.0	115.989	1.97	297322.673	241.879	39.553	18.767	1.571192049e6	1.288
9000.0	146.498	1.991	336046.785	246.442	37.836	17.049	1.807099542e6	1.286
10000.0	180.675	1.986	372961.362	250.333	35.979	15.193	2.047222929e6	1.287
11000.0	218.099	1.962	408052.021	253.679	34.211	13.425	2.29095485e6	1.289
12000.0	258.301	1.925	441490.549	256.589	32.676	11.89	2.537806546e6	1.292
13000.0	300.818	1.881	473549.464	259.156	31.484	10.698	2.787389971e6	1.296
14000.0	345.231	1.834	504545.723	261.453	30.59	9.804	3.039399948e6	1.3
15000.0	391.19	1.788	534806.189	263.541	29.996	9.21	3.293598228e6	1.304
16000.0	438.423	1.744	564646.464	265.467	29.722	8.936	3.549799968e6	1.308
17000.0	486.741	1.705	594357.51	267.269	29.744	8.958	3.80786255e6	1.312
18000.0	536.03	1.671	624196.974	268.974	29.964	9.178	4.067676383e6	1.315
19000.0	586.244	1.642	654383.656	270.606	30.448	9.662	4.329157371e6	1.318
20000.0	637.389	1.62	685094.498	272.181	39.3	18.514	4.59224074e6	1.321

**Table 26.** Thermodynamic properties of normal H<sub>2</sub>.

$T$ [K]	$Q_{int}$	$E_{int}/RT$ [J]	$H - H(0)$ [J mol <sup>-1</sup> ]	$S$ [J K <sup>-1</sup> mol <sup>-1</sup> ]	$C_p$ [J K <sup>-1</sup> mol <sup>-1</sup> ]	$C_v$ [J K <sup>-1</sup> mol <sup>-1</sup> ]	$-[G - H(0)]/T$ [J K <sup>-1</sup> mol <sup>-1</sup> ]	$\gamma$
5.0	2.28	0.0	103.931	39.472	20.786	0.0	51.859	1.667
10.0	2.28	0.0	207.861	53.88	20.786	0.0	247.797	1.667
15.0	2.28	0.0	311.792	62.308	20.786	-0.0	498.116	1.667
20.0	2.28	0.0	415.723	68.288	20.786	0.0	783.751	1.667
25.0	2.28	0.0	519.654	72.926	20.786	0.0	1095.646	1.667
30.0	2.28	0.0	623.585	76.716	20.786	0.0	1428.468	1.667
35.0	2.28	0.0	727.518	79.92	20.787	0.001	1778.693	1.667
40.0	2.28	0.0	831.461	82.696	20.791	0.005	2143.818	1.667
45.0	2.28	0.0	935.441	85.146	20.802	0.016	2521.971	1.667
50.0	2.28	0.0	1039.506	87.339	20.827	0.041	2911.705	1.666
60.0	2.28	0.002	1248.259	91.144	20.941	0.155	3721.536	1.666
70.0	2.281	0.006	1458.731	94.388	21.175	0.389	4566.442	1.664
80.0	2.284	0.014	1672.186	97.238	21.537	0.751	5441.706	1.661
90.0	2.29	0.026	1889.847	99.801	22.011	1.225	6343.964	1.656
100.0	2.298	0.041	2112.669	102.148	22.563	1.777	7270.725	1.649
110.0	2.309	0.06	2341.243	104.326	23.155	2.369	8220.08	1.641
120.0	2.323	0.082	2575.795	106.367	23.754	2.968	9190.508	1.632
130.0	2.34	0.106	2816.26	108.291	24.334	3.548	10180.745	1.623
140.0	2.361	0.131	3062.367	110.115	24.881	4.094	11189.711	1.613
150.0	2.384	0.157	3313.73	111.849	25.385	4.599	12216.458	1.603
200.0	2.54	0.287	4634.245	119.434	27.269	6.483	17589.625	1.56
150.0	2.384	0.157	3313.73	111.849	25.385	4.599	12216.458	1.603
298.15	2.964	0.487	7404.367	130.682	28.834	8.047	29079.567	1.503
300.0	2.973	0.49	7457.721	130.861	28.846	8.06	29306.112	1.503
350.0	3.224	0.561	8906.702	135.327	29.08	8.294	35547.806	1.485
400.0	3.488	0.616	10363.571	139.218	29.181	8.395	41997.824	1.473
450.0	3.761	0.66	11823.929	142.658	29.229	8.442	48630.664	1.463
500.0	4.039	0.696	13286.154	145.739	29.259	8.473	55426.21	1.455
600.0	4.609	0.75	16215.191	151.079	29.326	8.54	69443.696	1.444
700.0	5.191	0.791	19152.97	155.608	29.44	8.654	83952.266	1.437
800.0	5.782	0.823	22105.469	159.55	29.623	8.837	98882.88	1.43
900.0	6.381	0.852	25079.998	163.053	29.88	9.094	114184.769	1.425
1000.0	6.989	0.878	28083.68	166.217	30.204	9.418	129819.345	1.421
1100.0	7.608	0.903	31122.471	169.113	30.579	9.793	145756.449	1.416
1200.0	8.239	0.928	34200.737	171.792	30.99	10.204	161971.903	1.412
1300.0	8.883	0.953	37321.228	174.289	31.422	10.635	178445.876	1.408
1400.0	9.542	0.978	40485.298	176.634	31.86	11.074	195161.754	1.404
1500.0	10.217	1.003	43693.188	178.847	32.297	11.51	212105.359	1.399
2000.0	13.874	1.129	60353.995	188.419	34.278	13.492	299855.404	1.38
2500.0	18.083	1.248	77899.277	196.243	35.838	15.052	391921.882	1.364
3000.0	22.92	1.354	96138.376	202.89	37.077	16.291	487589.013	1.35
3500.0	28.448	1.45	114944.134	208.686	38.122	17.336	586356.362	1.339
4000.0	34.724	1.536	134239.943	213.838	39.043	18.257	687853.627	1.329
4500.0	41.805	1.615	153968.934	218.484	39.852	19.065	791795.791	1.321
5000.0	49.748	1.687	174065.773	222.719	40.508	19.722	897955.017	1.314
6000.0	68.431	1.809	214980.038	230.176	41.156	20.37	1.116191248e6	1.302
7000.0	91.097	1.899	256033.52	236.505	40.784	19.998	1.34130376e6	1.294
8000.0	117.857	1.954	296259.779	241.879	39.56	18.774	1.572254912e6	1.29
9000.0	148.594	1.977	334983.848	246.442	37.84	17.054	1.808162398e6	1.288
10000.0	182.999	1.973	371898.356	250.333	35.983	15.197	2.048285773e6	1.288
11000.0	220.648	1.95	406988.917	253.679	34.219	13.432	2.292017674e6	1.29
12000.0	261.068	1.914	440427.327	256.589	32.717	11.931	2.538869339e6	1.293
13000.0	303.791	1.871	472486.104	259.156	31.482	10.696	2.788452722e6	1.297
14000.0	348.397	1.825	503482.216	261.453	30.569	9.782	3.040462648e6	1.301
15000.0	394.537	1.78	533742.527	263.541	30.004	9.217	3.294660864e6	1.305
16000.0	441.939	1.736	563582.645	265.467	29.741	8.955	3.550862531e6	1.309
17000.0	490.413	1.697	593293.539	267.268	29.736	8.95	3.808925029e6	1.313
18000.0	539.849	1.664	623132.856	268.974	29.995	9.209	4.06873877e6	1.316
19000.0	590.199	1.636	653319.399	270.606	30.443	9.657	4.330219658e6	1.319
20000.0	641.473	1.613	684030.114	272.181	39.297	18.511	4.593302921e6	1.321

**Table 27.** Thermodynamic properties of ortho H<sub>2</sub>.

$T$ [K]	$Q_{int}$	$E_{int}/RT$ [J]	$H - H(0)$ [J mol <sup>-1</sup> ]	$S$ [J K <sup>-1</sup> mol <sup>-1</sup> ]	$C_p$ [J K <sup>-1</sup> mol <sup>-1</sup> ]	$C_v$ [J K <sup>-1</sup> mol <sup>-1</sup> ]	$-[G - H(0)]/T$ [J K <sup>-1</sup> mol <sup>-1</sup> ]	$\gamma$
5.0	3.0	0.0	103.931	41.756	20.786	0.0	63.277	1.667
10.0	3.0	0.0	207.861	56.164	20.786	0.0	270.633	1.667
15.0	3.0	0.0	311.792	64.592	20.786	0.0	532.37	1.667
20.0	3.0	0.0	415.723	70.572	20.786	0.0	829.423	1.667
25.0	3.0	0.0	519.654	75.21	20.786	0.0	1152.736	1.667
30.0	3.0	0.0	623.584	79.0	20.786	0.0	1496.976	1.667
35.0	3.0	0.0	727.515	82.204	20.786	0.0	1858.619	1.667
40.0	3.0	0.0	831.446	84.98	20.786	0.0	2235.16	1.667
45.0	3.0	0.0	935.377	87.428	20.786	0.0	2624.727	1.667
50.0	3.0	0.0	1039.308	89.618	20.786	0.0	3025.865	1.667
60.0	3.0	0.0	1247.182	93.408	20.789	0.003	3858.425	1.667
70.0	3.0	0.0	1455.125	96.613	20.802	0.016	4725.796	1.667
80.0	3.0	0.001	1663.318	99.393	20.842	0.056	5622.99	1.666
90.0	3.001	0.002	1872.131	101.853	20.93	0.144	6546.308	1.666
100.0	3.002	0.004	2082.135	104.065	21.083	0.297	7492.933	1.665
110.0	3.003	0.008	2294.057	106.085	21.315	0.529	8460.68	1.663
120.0	3.006	0.014	2508.698	107.952	21.627	0.84	9447.833	1.66
130.0	3.011	0.023	2726.839	109.698	22.013	1.227	10453.031	1.657
140.0	3.017	0.034	2949.171	111.346	22.462	1.676	11475.178	1.652
150.0	3.025	0.047	3176.238	112.912	22.958	2.171	12513.382	1.647
200.0	3.103	0.14	4390.077	119.878	25.561	4.775	17922.591	1.61
150.0	3.025	0.047	3176.238	112.912	22.958	2.171	12513.382	1.647
298.15	3.416	0.352	7069.282	130.738	28.461	7.675	29431.377	1.54
300.0	3.424	0.355	7121.959	130.914	28.486	7.7	29658.024	1.539
350.0	3.641	0.441	8559.265	135.345	28.941	8.155	35901.334	1.515
400.0	3.88	0.51	10011.739	139.223	29.13	8.344	42351.87	1.497
450.0	4.134	0.566	11470.509	142.66	29.21	8.424	48984.875	1.484
500.0	4.399	0.611	12932.172	145.74	29.253	8.467	55780.474	1.474
600.0	4.948	0.679	15860.941	151.079	29.325	8.539	69797.982	1.459
700.0	5.517	0.73	18798.687	155.608	29.44	8.653	84306.554	1.448
800.0	6.098	0.77	21751.181	159.55	29.623	8.837	99237.169	1.441
900.0	6.69	0.804	24725.709	163.053	29.88	9.094	114539.057	1.434
1000.0	7.294	0.835	27729.391	166.217	30.204	9.418	130173.634	1.428
1100.0	7.909	0.864	30768.183	169.113	30.579	9.793	146110.737	1.423
1200.0	8.537	0.892	33846.448	171.792	30.99	10.204	162326.192	1.418
1300.0	9.179	0.92	36966.94	174.289	31.422	10.635	178800.165	1.413
1400.0	9.836	0.948	40131.01	176.634	31.86	11.074	195516.042	1.409
1500.0	10.511	0.975	43338.899	178.847	32.297	11.51	212459.648	1.404
2000.0	14.173	1.108	59999.706	188.419	34.278	13.492	300209.693	1.383
2500.0	18.393	1.231	77544.988	196.243	35.838	15.052	392276.17	1.366
3000.0	23.248	1.34	95784.081	202.89	37.077	16.291	487943.302	1.352
3500.0	28.797	1.438	114589.782	208.686	38.122	17.335	586710.645	1.34
4000.0	35.096	1.526	133885.328	213.838	39.042	18.256	688207.888	1.331
4500.0	42.202	1.606	153613.51	218.484	39.849	19.063	792149.966	1.322
5000.0	50.173	1.678	173708.508	222.718	40.503	19.717	898308.966	1.315
6000.0	68.916	1.802	214614.043	230.174	41.144	20.357	1.116543844e6	1.303
7000.0	91.645	1.893	255650.45	236.501	40.76	19.974	1.34165289e6	1.295
8000.0	118.466	1.948	295852.244	241.871	39.533	18.746	1.572597596e6	1.29
9000.0	149.256	1.971	334547.337	246.43	37.81	17.024	1.808495266e6	1.288
10000.0	183.704	1.967	371431.338	250.318	35.952	15.166	2.048605493e6	1.288
11000.0	221.382	1.945	406492.024	253.661	34.191	13.405	2.292321206e6	1.29
12000.0	261.814	1.909	439902.437	256.569	32.688	11.902	2.53915404e6	1.293
13000.0	304.533	1.866	471935.664	259.134	31.454	10.668	2.788716353e6	1.297
14000.0	349.119	1.82	502908.834	261.43	30.545	9.758	3.040703339e6	1.301
15000.0	395.221	1.775	533148.787	263.516	29.974	9.188	3.294877066e6	1.305
16000.0	442.572	1.732	562971.041	265.441	29.735	8.949	3.551052967e6	1.309
17000.0	490.982	1.693	592666.488	267.241	29.721	8.935	3.809088657e6	1.313
18000.0	540.34	1.659	622492.742	268.946	29.99	9.204	4.068874749e6	1.317
19000.0	590.602	1.631	652668.607	270.577	30.434	9.648	4.330327328e6	1.319
20000.0	641.778	1.61	683371.061	272.152	39.29	18.504	4.59338178e6	1.322

**Table 28.** Thermodynamic properties of para H<sub>2</sub>.

$T$ [K]	$Q_{int}$	$E_{int}/RT$ [J]	$H - H(0)$ [J mol <sup>-1</sup> ]	$S$ [J K <sup>-1</sup> mol <sup>-1</sup> ]	$C_p$ [J K <sup>-1</sup> mol <sup>-1</sup> ]	$C_v$ [J K <sup>-1</sup> mol <sup>-1</sup> ]	$-[G - H(0)]/T$ [J K <sup>-1</sup> mol <sup>-1</sup> ]	$\gamma$
5.0	1.0	0.0	103.931	32.622	20.786	0.0	17.605	1.667
10.0	1.0	0.0	207.861	47.03	20.786	0.0	179.289	1.667
15.0	1.0	0.0	311.792	55.458	20.786	0.0	395.355	1.667
20.0	1.0	0.0	415.723	61.437	20.786	0.0	646.735	1.667
25.0	1.0	0.0	519.654	66.076	20.786	0.0	924.377	1.667
30.0	1.0	0.0	623.585	69.865	20.787	0.001	1222.945	1.667
35.0	1.0	0.0	727.525	73.07	20.79	0.004	1538.917	1.667
40.0	1.0	0.0	831.508	75.847	20.806	0.02	1869.79	1.667
45.0	1.0	0.001	935.632	78.3	20.85	0.064	2213.703	1.666
50.0	1.0	0.002	1040.099	80.501	20.947	0.161	2569.224	1.666
60.0	1.001	0.009	1251.492	84.354	21.398	0.612	3310.871	1.663
70.0	1.003	0.025	1469.549	87.713	22.291	1.505	4088.379	1.656
80.0	1.009	0.054	1698.789	90.773	23.621	2.835	4897.857	1.644
90.0	1.017	0.097	1942.994	93.647	25.255	4.469	5736.931	1.626
100.0	1.031	0.151	2204.272	96.398	27.003	6.217	6604.1	1.606
110.0	1.049	0.215	2482.799	99.052	28.677	7.891	7498.282	1.583
120.0	1.071	0.283	2777.086	101.611	30.136	9.35	8418.531	1.561
130.0	1.099	0.354	3084.521	104.071	31.298	10.511	9363.887	1.539
140.0	1.131	0.423	3401.955	106.423	32.136	11.349	10333.31	1.52
150.0	1.167	0.488	3726.206	108.66	32.666	11.88	11325.683	1.503
200.0	1.393	0.727	5366.75	118.102	32.393	11.607	16590.726	1.449
150.0	1.167	0.488	3726.206	108.66	32.666	11.88	11325.683	1.503
298.15	1.937	0.892	8409.623	130.514	29.951	9.165	28024.137	1.418
300.0	1.947	0.894	8465.01	130.699	29.927	9.141	28250.377	1.418
350.0	2.24	0.919	9949.013	135.275	29.497	8.711	34487.222	1.413
400.0	2.535	0.933	11419.066	139.201	29.333	8.547	40935.684	1.411
450.0	2.831	0.944	12884.19	142.653	29.283	8.497	47568.031	1.409
500.0	3.128	0.951	14348.103	145.738	29.278	8.492	54363.419	1.408
600.0	3.725	0.963	17277.941	151.079	29.329	8.542	68380.839	1.406
700.0	4.324	0.973	20215.82	155.608	29.44	8.654	82889.401	1.404
800.0	4.928	0.983	23168.333	159.55	29.623	8.837	97820.014	1.403
900.0	5.536	0.994	26142.863	163.053	29.88	9.094	113121.903	1.401
1000.0	6.151	1.006	29146.545	166.217	30.204	9.418	128756.479	1.399
1100.0	6.774	1.019	32185.337	169.113	30.579	9.793	144693.583	1.397
1200.0	7.406	1.034	35263.602	171.792	30.99	10.204	160909.037	1.395
1300.0	8.051	1.051	38384.094	174.289	31.422	10.635	177383.01	1.392
1400.0	8.709	1.069	41548.164	176.634	31.86	11.074	194098.888	1.389
1500.0	9.382	1.089	44756.054	178.847	32.297	11.511	211042.494	1.386
2000.0	13.015	1.193	61416.861	188.419	34.278	13.492	298792.538	1.371
2500.0	17.181	1.299	78962.144	196.243	35.838	15.051	390859.016	1.357
3000.0	21.964	1.397	97201.262	202.89	37.077	16.291	486526.149	1.345
3500.0	27.428	1.486	116007.188	208.686	38.122	17.336	585293.51	1.335
4000.0	33.632	1.568	135303.791	213.838	39.047	18.26	686790.847	1.326
4500.0	40.634	1.644	155035.207	218.485	39.859	19.073	790733.265	1.318
5000.0	48.493	1.713	175137.568	222.721	40.522	19.736	896893.167	1.311
6000.0	66.995	1.831	216078.024	230.183	41.192	20.405	1.11513346e6	1.3
7000.0	89.472	1.919	257182.729	236.52	40.847	20.061	1.340256372e6	1.292
8000.0	116.05	1.972	297482.384	241.903	39.641	18.855	1.57122686e6	1.288
9000.0	146.624	1.994	336293.379	246.476	37.931	17.145	1.807163794e6	1.286
10000.0	180.9	1.99	373299.41	250.377	36.071	15.285	2.047326615e6	1.287
11000.0	218.462	1.966	408479.598	253.731	34.302	13.516	2.29110708e6	1.288
12000.0	258.842	1.93	442001.997	256.649	32.799	12.012	2.538015238e6	1.292
13000.0	301.576	1.887	474137.426	259.222	31.549	10.763	2.787661831e6	1.295
14000.0	346.243	1.84	505202.36	261.525	30.652	9.865	3.039740575e6	1.299
15000.0	392.49	1.794	535523.749	263.617	30.079	9.293	3.294012259e6	1.304
16000.0	440.045	1.75	565417.46	265.546	29.776	8.99	3.550291223e6	1.308
17000.0	488.713	1.711	595174.689	267.35	29.787	9.0	3.808434146e6	1.311
18000.0	538.38	1.676	625053.198	269.058	30.023	9.237	4.068330833e6	1.315
19000.0	588.994	1.648	655271.777	270.692	30.442	9.656	4.329896651e6	1.318
20000.0	640.561	1.625	686007.275	272.268	39.406	18.62	4.593066343e6	1.32